AD-E 300 291

(12) LEVEL II SC

DNA 4418F

ADA058437

SIMULATION OF PLANE UNDERWATER SHOCK WAVES USING AN ARRAY OF POINT VOLUME SOURCES

SRI International
333 Ravenswood Avenue
Menlo Park, California 94025

1 FEBRUARY 1978

Final Report for Period 26 March 1973—30 January 1978

CONTRACT No. DNA 001-73-C-0208

DDC

RECEIVED

SEP 8 1978

B

Prepared for
Director
DEFENSE NUCLEAR AGENCY
Washington, D. C. 20305

DDC FILE COPY

78 06 29 008

Destroy this report when it is no longer
needed. Do not return to sender.

(18) DNA, SBIE

(19) REPORT DOCUMENTATION PAGE		READ INSTRUCTIONS BEFORE COMPLETING FORM
1. REPORT NUMBER DNA 4418F AD-E300 291	2. GOVT ACCESSION NO.	3. RECIPIENT'S CATALOG NUMBER
4. TITLE (and Subtitle) SIMULATION OF PLANE UNDERWATER SHOCK WAVES USING AN ARRAY OF POINT VOLUME SOURCES.		5. TYPE OF REPORT & PERIOD COVERED Final Report for Period 26 Mar 73—30 Jan 78
		6. PERFORMING ORG. REPORT NUMBER PYU-2553
7. AUTHOR(s) C. M. Romander G. R. Abrahamson, Project Supervisor		8. CONTRACT OR GRANT NUMBER(s) DNA 001-73-C-0208
9. PERFORMING ORGANIZATION NAME AND ADDRESS SRI International 333 Ravenswood Avenue Menlo Park, California 94025		10. PROGRAM ELEMENT, PROJECT, TASK AREA & WORK UNIT NUMBERS NWET Subtask L02AAXYX971-01
11. CONTROLLING OFFICE NAME AND ADDRESS Director Defense Nuclear Agency Washington, D.C. 20305		12. REPORT DATE 1 FEB 78
		13. NUMBER OF PAGES 80
14. MONITORING AGENCY NAME & ADDRESS(if different from Controlling Office)		15. SECURITY CLASS (of this report) UNCLASSIFIED
		15a. DECLASSIFICATION/DOWNGRADING SCHEDULE

16. DISTRIBUTION STATEMENT (of this Report)

Approved for public release; distribution unlimited.

17. DISTRIBUTION STATEMENT (of the abstract entered in Block 20, if different from Report)

18. SUPPLEMENTARY NOTES

This work sponsored by the Defense Nuclear Agency under RDT&E RMSS
Code B344073462 L02AAXYX97101 H2590D.

19. KEY WORDS (Continue on reverse side if necessary and identify by block number)

20. ABSTRACT (Continue on reverse side if necessary and identify by block number)

Experiments were conducted to test the concept of using point volume sources
in a plane array to produce a plane shock wave in water that would simulate
the shock wave from a nuclear explosion. The point volume sources were
designed to produce gas volume at a constant rate, thereby producing a uni-
form shock wave. The volume sources consisted of a high pressure reservoir
of explosive product gases and an orifice area that increases with time as ⟶ next page

DD FORM 1473 EDITION OF 1 NOV 65 IS OBSOLETE
1 JAN 73

410 281 78 06 29 008

20.   ABSTRACT (Continued)

cont.

the pressure in the reservoir decreases to maintain a constant rate of volume generation at each source.

The tests consisted of two 20 x 20 ft array tests consisting of 100 point sources, and seven auxiliary tests. The tests showed that the point-source-to-plane wave concept is valid; however, the waves from the point sources did not superpose linearly due to interaction of the bubbles.

Of the problems encountered during the tests, all have a direct solution, except possibly the drag from the residue of the explosion products on the motion of the piston that controls the orifice area. Successful implementation of the suggested design modifications will make the array pipes and valves more watertight and thereby reduce the effect of the residue from the explosion products.

SUMMARY AND CONCLUSIONS

Summary. The objective of the experiments described here was to test the concept of using point volume sources in a plane array to produce a plane shock wave in water that would simulate the shock wave from a nuclear explosion. The point volume sources were designed to produce gas volume at a constant rate, thereby producing a uniform shock wave. The volume sources consisted of a high pressure reservoir of explosive product gases, and an orifice area that increases with time as the pressure in the reservoir decreases, to maintain a constant rate of volume generation at each source. The tests showed that the point-source-to-plane-wave concept is valid. However, the waves from the point sources did not superimpose linearly due to interaction of the bubbles.

The tests were conducted over a period of 3 weeks, consisting of 1 week for preparation and 2 weeks for testing. This includes the time for assembly of 100 valves from the basic parts, assembly of the valves and pipes into an array, installation of the explosive, and firing of 2 full array tests (100 point sources) and 7 auxiliary tests. The team consisted of 3 full-time UERD technicians and 5 support technicians who helped from time to time, a UERD engineer, and an engineer and technician from SRI.

In the performance of the tests, the following operational aspects went well:

- Valves were assembled quickly and efficiently.
- Arrays were assembled with minimum trouble.
- The array was easy to load with explosive and to detonate.

The following problems were encountered:

- Most of the valves needed reconditioning between tests. It was found that the explosion products mixed with water to form a waxy substance that tends to inhibit the motion of the piston that controls the orifice area. The return spring was not strong enough to push the piston back consistently, especially with the residue from the explosive impeding piston motion. This can be corrected in part by using a stronger spring, but elimination or reduction of the residue is necessary for efficient repeat testing.

- The pins that hold the baffle plate in place were too short - when screwed in they provided minimal resistance to motion of the baffle plate. This can be remedied by making the pins longer.

- The O-ring between the baffle and base plate was blown out on several valves, allowing water to leak into the array pipes. To prevent this, the O-ring grooves should be made deeper.

- About 15% of the rubber bladders folded back on themselves providing a large leak path for water to enter the array pipes. This could be prevented by making the bladders longer.

- A manufacturing error led to the valves not seating in the proper initial position, giving an initial orifice area that was one-third greater than the design area. This produced a perturbation on the pulse shape, but did not affect the overall outcome of the tests.

- Some of the reservoir pipes failed below the design loads. The design loads for the reservoir pipes were based on extensive explosive tests of the pipes in air. The pipes were of high strength steel and the strength is sensitive to the heat treatment. It was found that the design loads can be carried for pipes with a hardness of 34 to 38 R_c. The pipes used in the array tests were found to have a hardness of 40 R_c.

All of these problems, except possibly the residue from the explosive products, have a direct solution that, we believe, can be readily implemented. Successful implementation of the design modifications suggested above will make the array pipes and valves more watertight and thereby reduce the effect of the residue from the explosion products.

Conclusions. The array tests were carried out successfully within a reasonable period of time and the measurements show that plane shock waves were obtained (Figure 19). The nonuniformity in the wave is attributed to the source characteristics and can be reduced to an acceptable level by adjusting the area-time relation of the orifice (Figure 20.

Further refinement of the valving techniques described in this report should be deferred until the current work with coiled-charge point volume sources has been evaluated (see Preface).

Should the array technique be developed further, a pipe of about two feet in diameter should be used instead of arrays. This would greatly reduce the cost and time involved.

PREFACE

This report describes the culmination of a developmental program
started in 1973. The goal of the program was to develop a shock curtain
that would produce a plane underwater shock wave that could be used to
determine the equipment damage that submarines and submarine components
are likely to suffer in nuclear explosions. As indicated in this report,
a practical shock curtain was developed that is suitable when the number
of tests is high enough to justify the hardware investment.

During the final tests of the shock curtain, the concept of a chock
block consisting of strands of explosive extending normal to the desired
shock front was conceived at the Navy's Underwater Explosive Research
Division (UERD). This concept was tested and it was found that the inter-
action between adjacent strands resulted in cooling of the explosion
product gases, thus severely restricting the pulse durations obtainable.
To eliminate the quenching problem, it was proposed that the strands of
explosive be wound into a coil to be used as point volume sources in
place of the valves used in the shock curtain development. This would
provide an attractive alternative to the shock curtain.

3

Conversion factors for U.S. customary to metric (SI) units of measurement.

To Convert From	To	Multiply By
angstrom	meters (m)	1.000 000 X E –10
atmosphere (normal)	kilo pascal (kPa)	1.013 25 X E +2
bar	kilo pascal (kPa)	1.000 000 X E +2
barn	meter^2 (m^2)	1.000 000 X E –28
British thermal unit (thermochemical)	joule (J)	1.054 350 X E +3
calorie (thermochemical)	joule (J)	4.184 000
cal (thermochemical)/cm^2	mega joule/m^2 (MJ/m^2)	4.184 000 X E –2
curie	*giga becquerel (GBq)	3.700 000 X E +1
degree (angle)	radian (rad)	1.745 329 X E –2
degree Fahrenheit	degree kelvin (K)	$t_K = (t°f + 459.67)/1.8$
electron volt	joule (J)	1.602 19 X E –19
erg	joule (J)	1.000 000 X E –7
erg/second	watt (W)	1.000 000 X E –7
foot	meter (m)	3.048 000 X E –1
foot-pound-force	joule (J)	1.355 818
gallon (U.S. liquid)	meter^3 (m^3)	3.785 412 X E –3
inch	meter (m)	2.540 000 X E –2
jerk	joule (J)	1.000 000 X E +9
joule/kilogram (J/kg) (radiation dose absorbed)	Gray (Gy)	1.000 000
kilotons	terajoules	4.183
kip (1000 lbf)	newton (N)	4.448 222 X E +3
kip/inch^2 (ksi)	kilo pascal (kPa)	6.894 757 X E +3
ktap	newton-second/m^2 (N-s/m^2)	1.000 000 X E +2
micron	meter (m)	1.000 000 X E –6
mil	meter (m)	2.540 000 X E –5
mile (international)	meter (m)	1.609 344 X E +3
ounce	kilogram (kg)	2.834 952 X E –2
pound-force (lbs avoirdupois)	newton (N)	4.448 222
pound-force inch	newton-meter (N·m)	1.129 848 X E –1
pound-force/inch	newton/meter (N/m)	1.751 268 X E +2
pound-force/foot^2	kilo pascal (kPa)	4.788 026 X E –2
pound-force/inch^2 (psi)	kilo pascal (kPa)	6.894 757
pound-mass (lbm avoirdupois)	kilogram (kg)	4.535 924 X E –1
pound-mass-foot^2 (moment of inertia)	kilogram-meter^2 (kg·m^2)	4.214 011 X E –2
pound-mass/foot^3	kilogram/meter^3 (kg/m^3)	1.601 846 X E +1
rad (radiation dose absorbed)	**Gray (Gy)	1.000 000 X E –2
roentgen	coulomb/kilogram (C/kg)	2.579 760 X E –4
shake	second (s)	1.000 000 X E –8
slug	kilogram (kg)	1.459 390 X E +1
torr (mm Hg, 0° C)	kilo pascal (kPa)	1.333 22 X E –1

*The becquerel (Bq) is the SI unit of radioactivity; 1 Bq = 1 event/s.
**The Gray (Gy) is the SI unit of absorbed radiation.

A more complete listing of conversions may be found in "Metric Practice Guide E 380-74," American Society for Testing and Materials.

CONTENTS

ILLUSTRATIONS

<u>Figure</u>

6

ILLUSTRATIONS (continued)

TABLES

I INTRODUCTION

Background

Damage to submarines from nearby explosions is generally divided into two types: hull damage and equipment damage. Hull damage consists of damage to the basic structure of the submarine and affects overall seaworthiness. Equipment damage encompasses damage to machinery, weapons, propulsion, components, and other items that are not part of the basic hull structure. It affects primarily mobility and fire power capabilities, which determine mission effectiveness. For shallow depths, submarine survivability under nuclear attack is currently limited by equipment damage. Moreover, since equipment tends to become more complex as time goes on, this situation is not likely to change. Therefore, as long as submarines continue to grow in importance as part of the strategic force, economical methods for testing the vulnerability of submarines to equipment damage and for specification testing of new equipment will become increasingly important.

In the engulfment of a submarine by an underwater shock wave from a nuclear explosion, the submarine is accelerated and reaches 90% of the water particle velocity by the time engulfment is complete.[1] Thus, testing a submarine for equipment damage from nuclear attack requires a volume of water somewhat larger than the submarine, moving at an approximately uniform velocity.

Conventional methods for testing submarines or large components of submarines for equipment damage from nuclear attack use large underwater chemical explosions and rely on geometric divergence to reduce the intensity of the shock wave to the desired level and obtain a wavefront

---

[1]
R. D. Mindlin and H. H. Bleich, "Response of an Elastic Cylindrical Shell to a Transverse, Step Shock Wave," J. Appl. Mech., 189 (June 1953).

9

flat enough to simulate a shock wave from a nuclear explosion. Since only a small fraction of the wavefront area is used, most of the energy of the explosive is wasted.

Objective

The objective of the work described in this report was to develop and test an alternative method for producing underwater shock waves with nuclear characteristics for testing submarines or large components of submarines for equipment damage. The method uses controlled venting of explosive gases over a vertical plane in the water to produce a plane wave of the required intensity, area, and duration. Since it does not rely on geometric divergence, the amount of explosive required is less than that required by conventional methods. This reduction in explosive greatly reduces the environmental disturbance. Hence, tests can be performed in more convenient locations, simplifying personnel support and instrumentation problems. In addition, turnaround time and overall cost are less.

Approach

The method we used to produce plane underwater shock waves involves a plan array of volume sources, spaced close enough together that the waves from the individual volume sources coalesce to produce a plane wave before reaching the test object, as shown in Figure 1. The development consisted of three phases: a preliminary study to determine geometric and physical restrictions and to set performance standards; a developmental program to design, build, and test a single volume source that met the performance standards; and a field test program to construct and test a small array of volume sources.

POINT VOLUME SOURCES
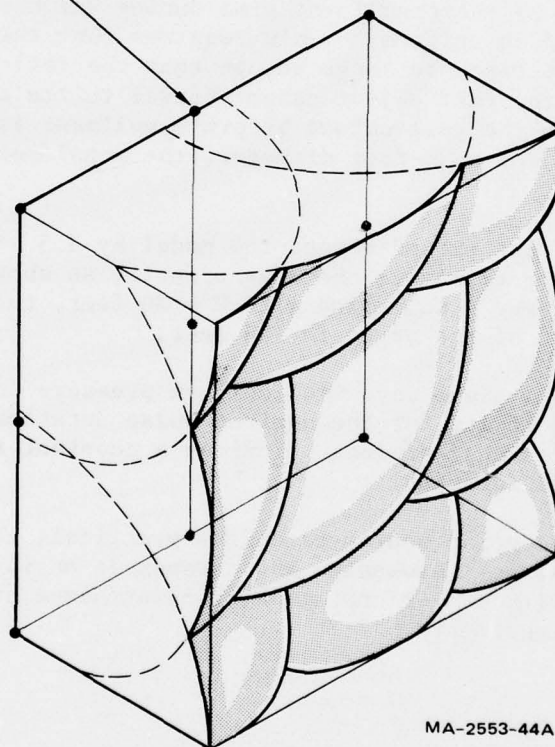
MA-2553-44A

FIGURE 1   PLANE WAVE GENERATED BY AN
ARRAY OF POINT VOLUME
SOURCES

11

The preliminary study was performed early in the program and results were presented in an interim report.[2] The following geometric and physical restraints and performance requirements for the array concept were determined:

- If D is the engulfment distance (target diameter), the resulting minimum standoff distance is d = D/2 (see Figure 2). The minimum standoff distance is determined by the engulfment time during which the wave should be uniform.* This requires that the standoff distance be large enough that the reflected wave from the test object cannot travel to the array and back to the test object before engulfment is complete. For a 30-foot diameter, the engulfment time is 6 ms.

- The array must extend beyond the model by 3.5 standoff distances to eliminate the edge effects, as shown in Figure 2. For a submarine with D = 30 feet, the verticle dimension L of the array is 105 feet.

- To produce a plane wave with uniform pressure and particle velocity for the desired pulse duration, each point source must produce volume at a constant rate for the desired duration.

- To make the point source technique practical, each point source must be inexpensive and expendable or it must be reusable without performing major maintenance or repair between experiments.

---

[2]G. R. Abrahamson, D. J. Cagliostro, and C. M. Romander, "Simulation of Underwater Shock Waves from Nuclear Explosions," Interim Report for Period 26 March 1973 to 31 October 1974, Contract DNA001-73-C-0208 (November 1974).

*At the onset of the program it was assumed that a wave that is uniform during engulfment and that has a gradual decay would be adequate for most applications, since the hull achieves 90% of the water particle velocity during engulfment. For equipment with response times longer than one engulfment time, waves of longer duration would be required.
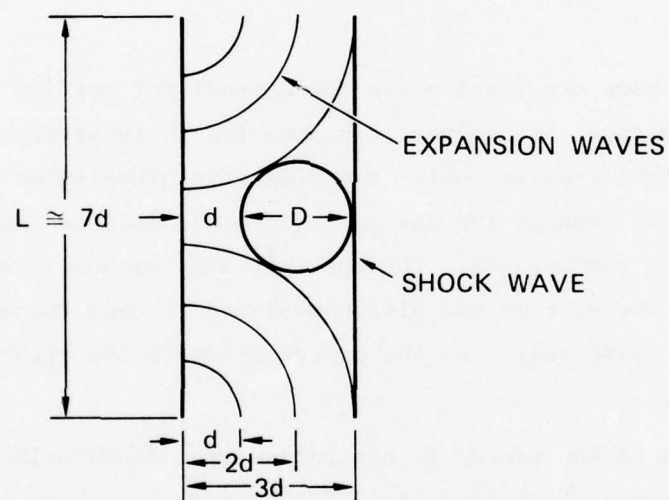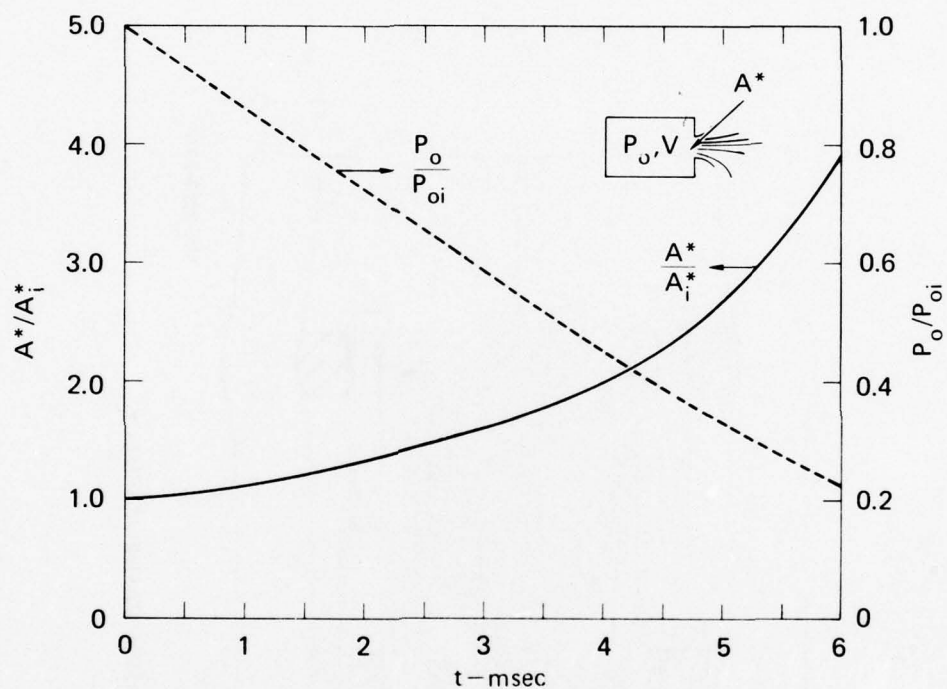
FIGURE 2   RELATIONSHIP BETWEEN ARRAY SIZE
           AND OBJECT SIZE

MA-2553-29

13

The key physical requirement is that each point source of the array must produce volume at a constant rate. To accomplish this, we used controlled venting of explosion product gases. The explosive is detonated to produce a reservoir of high pressure gas, which is allowed to flow into the water in such a way that volume is generated at a constant rate. Because the pressure in the reservoir decreases as gas escapes, the orifice through which the gases escape must increase with time, as indicated in Figure 3. Devising a suitable means of increasing the orifice area as the pressure decreases in the reservoir was the major design problem in this work. (See Appendix A for a detailed discussion of the development.)

Figure 4 shows the final design of a practical orifice control valve for use in an array. The valves are connected to reservoir pipes on the left. The explosive gases inside the reservoir pipes enter the valve from the left and push on the piston. Slots machined in the wall of the piston allow for gas exhaust. The gas initially exhausts through the narrow part of the slot in the piston wall and through the annular opening in the valve wall. As the piston moves to the right, the exhaust area increases.

The motion of the piston is controlled by a fluid-orifice system. As the piston moves, it forces fluid (oil) through several orifices in the orifice plate. The motion of the piston is controlled by adjusting the size of the orifices. After passing through the orifice plate, the fluid compresses a volume of closed-cell foam until the piston comes to rest. Then a spring in the fluid chamber expands and pushes the piston back to its original position, and the foam expands and displaces the fluid back into the fluid chamber. At this point, the valve has returned to its original condition and is ready for another test. This recocking feature makes the valve practical.
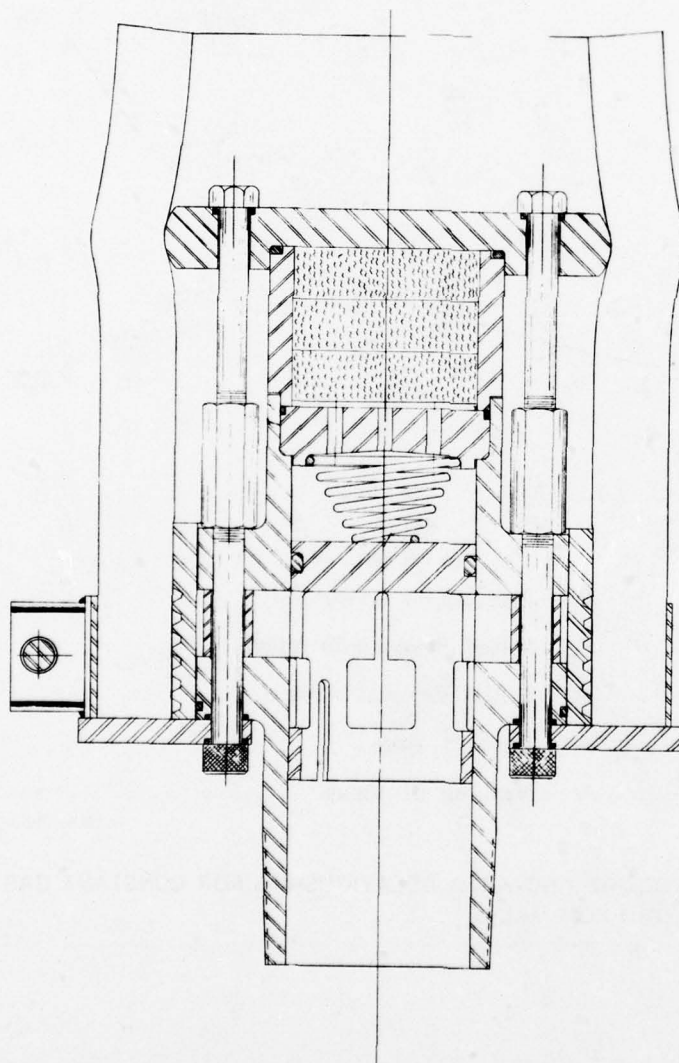
14

FIGURE 3   PRESSURE AND AREA RELATIONSHIPS FOR CONSTANT GAS
FLOW FROM VALVE

MA-2553-35A

15

MA-2553-57A

FIGURE 4   ORIFICE VALVE ASSEMBLY

To demonstrate the operation of the valve on a laboratory scale, experiments were conducted in a 22-foot-long, 6-inch-diameter steel pipe as shown in Figure 5. This pipe simulates a long, narrow column of water perpendicular to an array of these valves. Therefore, the pulse shape measured in the pipe will be similar to the pulse expected from an array but the amplitude will be greater. The valve was connected to a 2-foot-long, 2-inch-diameter pipe containing 2-foot-long charges of Primacord. The valve and connecting pipe were placed in the breech end of the 6-inch-diameter pipe.

Figure 6 shows a pressure record made approximately 6 feet from the valve (8.1 feet from the breech). The pressure from the source (400 grains of explosive) rises suddenly to a peak pressure of about 900 psi (62 bars) and remains nearly constant for 6 ms, after which a relief wave from a free surface at the downstream end of the pipe arrives at the measurement point, reducing the pressure to one atmosphere. This pressure exceeds the useful level of the array. Although the explosive charge is reasonable for the pipe and valve, the cross-sectional area of the 6" pipe is about 16 times smaller (charge density about 16 times larger) than expected for a 2-foot source spacing. By scaling the charge density to prototype dimensions and using calibration data for the explosive obtained in previous work, [2,3] we would expect a charge density of 6.5 grains/ft^2 and a peak pressure of 260 psi. Results of additional experiments of this type are given in Appendix A.

The final phase in the development of the array concept to produce plane underwater shock waves was to test an array of point sources. The remainder of this report describes the array test using the valves described above.

_____

[3]D. J. Cagliostro, A. L. Florence, G. R. Abrahamson, and G. Nagumo, "Characterization of an Energy Source for Modeling Hypothetical Core Disruptive Accidents in Nuclear Reactors," Nuclear Engineering and Design, 27, 94-105 (March 1974).

17
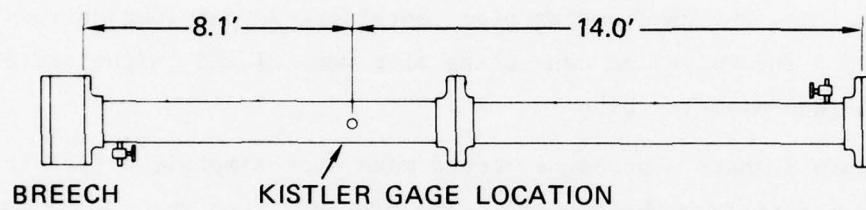
(a) TEST FIXTURE
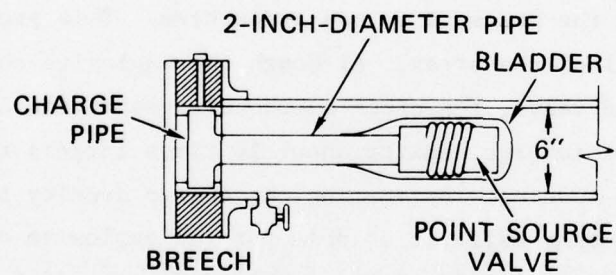
(b) TEST CONFIGURATION OF POINT VOLUME SOURCE

MA-2553-45A

FIGURE 5   EXPERIMENTAL SETUP TO TEST VALVES

18

900 psi

1 msec

250 psi

CHARGE = 400 grains
PRIMACORD
P at 8.1 feet
(6 feet from valve)

MP-2553-50A

FIGURE 6   PRESSURE PULSE FROM PIPE EXPERIMENT OF VALVE

II   EXPERIMENTAL ARRANGEMENT

To demonstrate the array technique for producing plane shock waves in water by superposition of spherical waves from point sources, we tested a 10 x 10 array of point sources spaced uniformly at 2-foot spacing (100 point sources in a 20 foot x 20 foot array), as shown in Figure 7. The primary objectives of the test (UERD Shot No. 8820) were to:
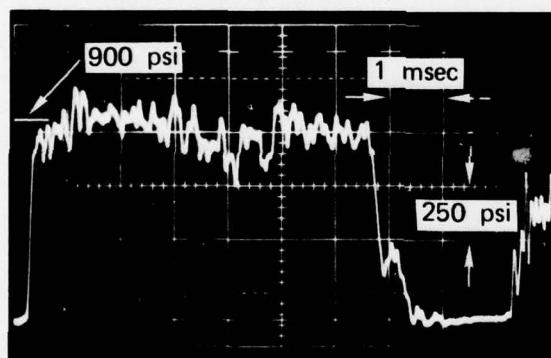
   (1)   Validate the point-source-to-plane-wave concept.

   (2)   Evaluate the overall system in terms of practical utility.

   (3)   Determine any changes needed in the orifice area-time relation.

The arrangement of Figure 8 was used to detonate the explosive. This detonation scheme produces a plane wave that is tilted from the array, as shown in Figure 9.

The instrumentation layout for the main test is shown in Figure 10. One line of transducers extends along the central normal of the array, and a second line extends out to one side. In all, there were 12 pressure transducers[*] and 2 velocity meters.[†] All the instrumentation work was done by UERD personnel under the direction of Mr. John Gordon. Excellent data were obtained.

In addition to the main test, several auxiliary tests were performed. These were:

   (1)   A single valve test to obtain the pulse shape for one source
         (Test 8815). A check on the valve operation was made by com-
         paring data from this test with results from a similar test
         performed during the developmental program. The pressure
         pulse from a single source provides data for use in super-
         position calculations.

---

[*] Tourmaline Crystal gage manufactured by the Naval Surface Weapons Center

[†] Magnetic field device designed and built by UERD.
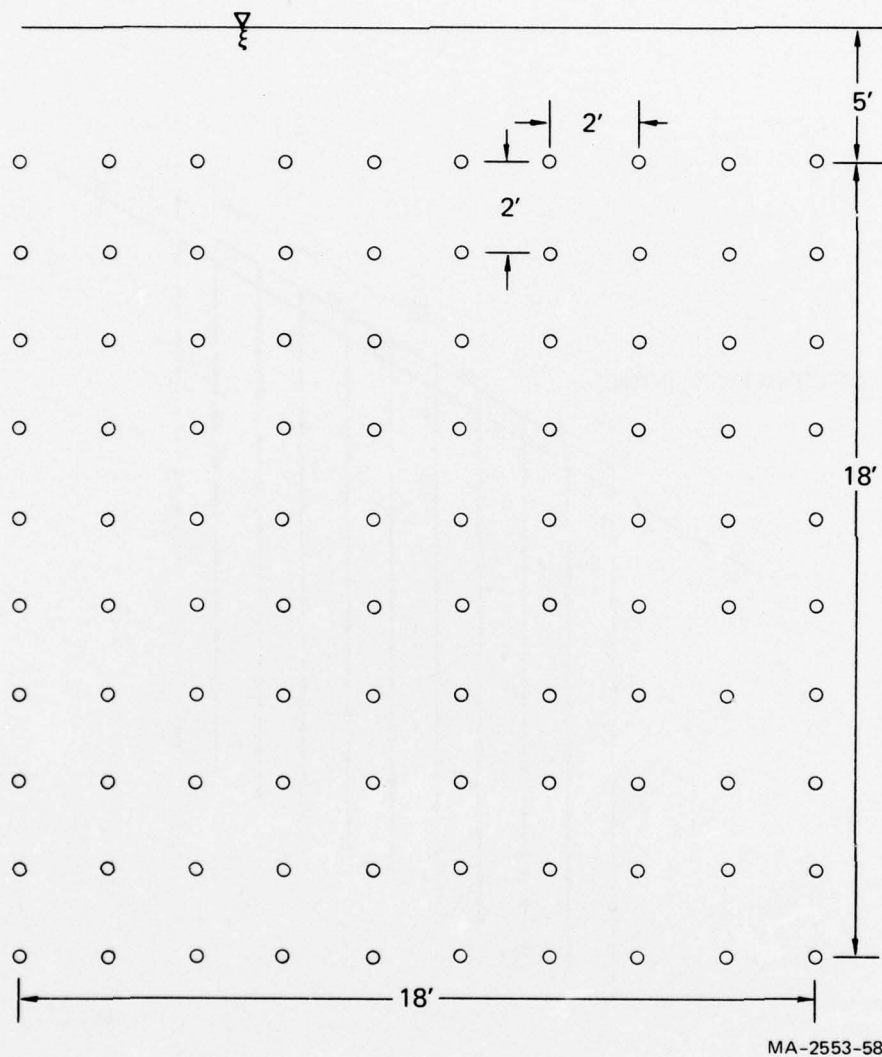
MA–2553–58

FIGURE 7   PLANE ARRAY OF 100 POINT SOURCES

21

DETONATION POINT

1'

5'

18'

18'
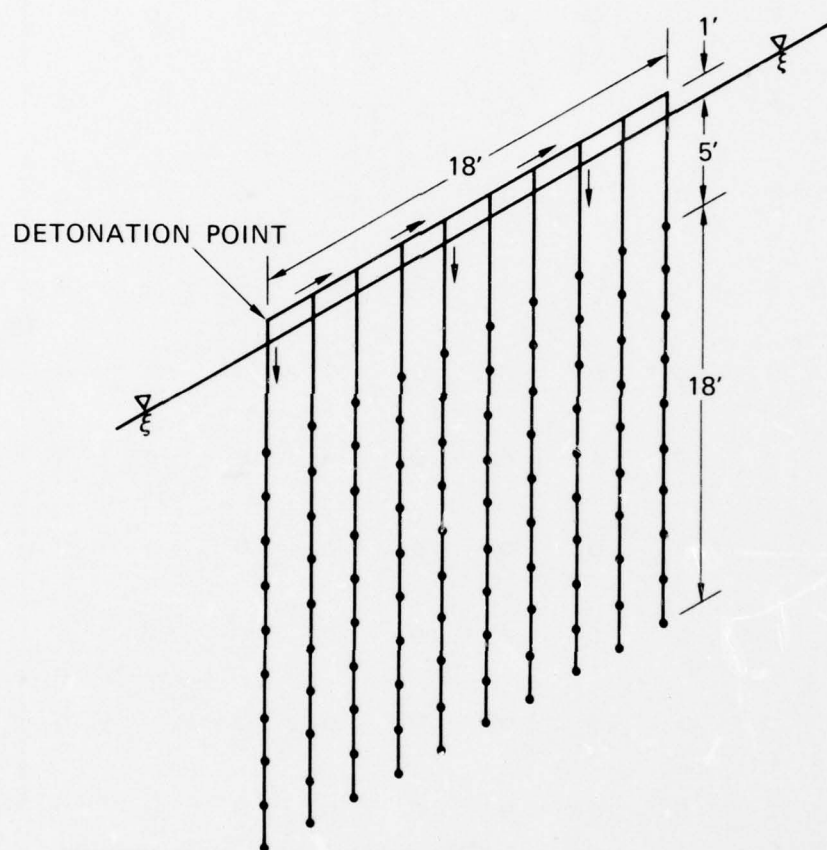
MA-2553-59

FIGURE 8   DETONATION SCHEME

22
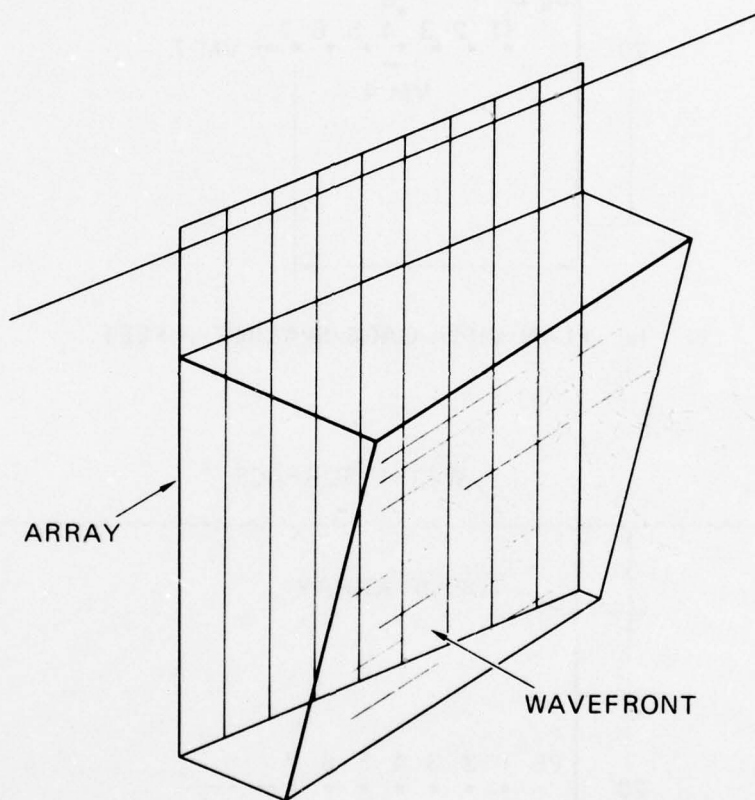
ARRAY

WAVEFRONT

MA-2553-60

FIGURE 9   WAVEFRONT TILT

23
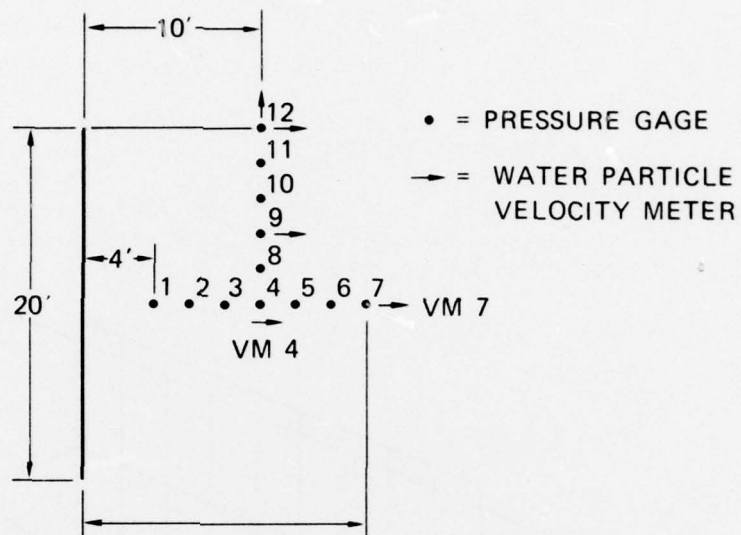
(a) PLAN VIEW; GAGE SPACING, 2 FEET
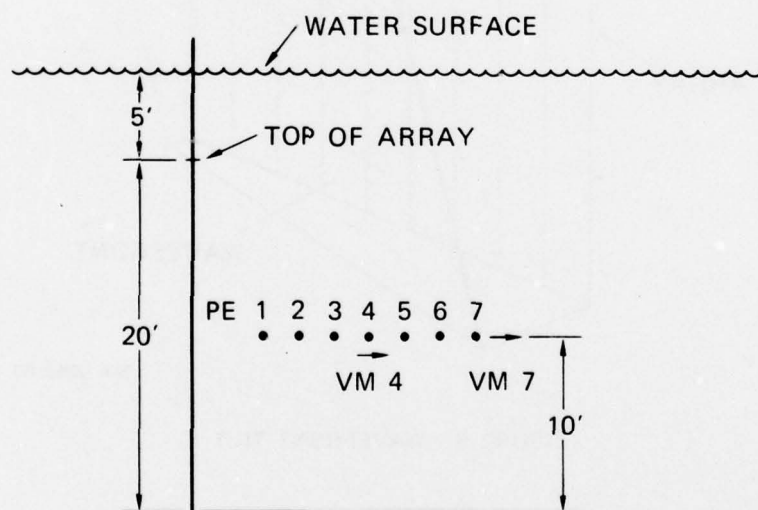
(b) ELEVATION

MA-2553-61

FIGURE 10   TEST GEOMETRY AND INSTRUMENTATION

24

(2) A single line element test (Test 8819). This element
consisted of 10 valves connected to a 20-foot-long array
pipe. This test was designed to evaluate handling and
operational procedures and to provide data for a simple
case to check superposition.

(3) A series of bare Primacord experiments designed to
evaluate an alternative shock generation technique (shock
block, Tests 8821, 8822, 8825, and 8826).

All the test results are contained in a report by UERD.[4] In
addition, UERD filmed key tests.

---

[4]J. D. Gordon, "Shock Curtain Evaluation Test Results," UERD Report to
DNA, Serial No. 1770-128 (11 November 1976).

III   ARRAY TEST RESULTS

The pressure records from the main array test for the gage line extending along the central normal to the array are shown in Figure 11. The records are arranged in order of decreasing distance from the array. The spacing of the records is proportional to the spacing between gage locations. Time is measured from the start of detonation.

The pressure records show an initial rise, followed by a decay and a second rise, and then a final decay. The rise time to the initial peak is about 0.5 ms for all records. The rise time and two-peak characteristic are related to the pulse shape for the individual sources; this is discussed below (Figure 21).[*]

As indicated in Figure 11, the wavefront arrival times correspond to a wave velocity in water of 5000 ft/s (1525 m/s), in agreement with the handbook value.

The line labeled "rarefaction arrival time" is the time at which the first edge rarefaction arrives at the gage location. The calculation for the arrival of the first rarefaction is given in Appendix B. The time between the arrival of the wavefront and the arrival of the edge rarefaction decreases with distance from the array, as expected. As indicated in Table 1 and Figure 12 (solid line), this difference ranges from 1.035 ms for the gage 4 feet from the array, to 0.209 ms for the gage 16 feet from the array. The wave should be plane between the time of arrival of the wave and the time of arrival of the first edge rarefaction.

Arrival of surface cutoff is denoted by the arrows labeles t_s in Figure 11. (See Appendix B for surface cutoff calculations.) Surface cutoff always arrives after the edge rarefaction. No distinguishable feature of the pulse shape appears to be related to surface cutoff arrival.

---

[*]As indicated in the discussion of Figure 21 (page 42), it appears possible to improve the pulse shape to obtain a more nearly uniform pulse, which would be more representative of the desired shape.
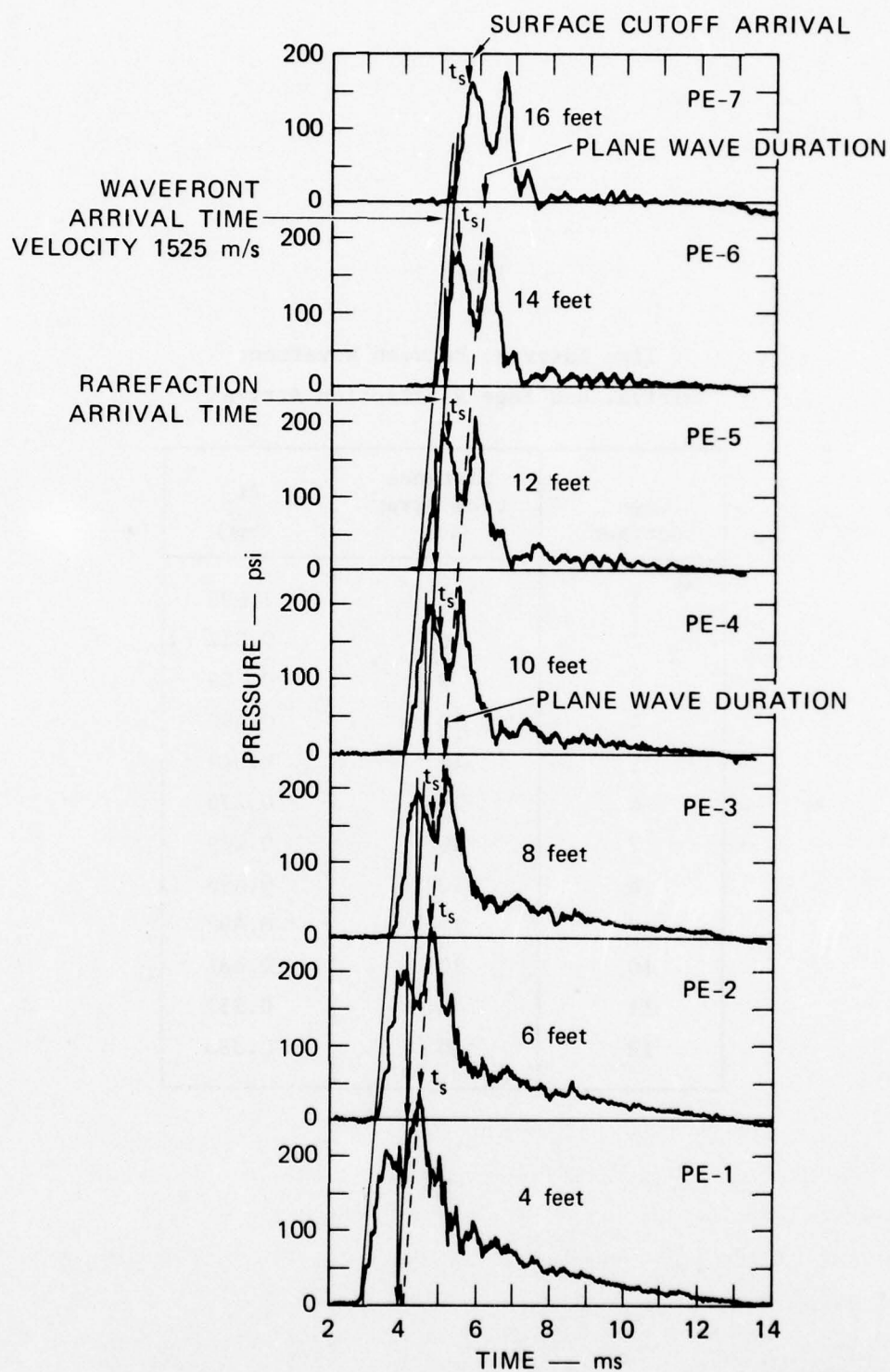
FIGURE 11   PRESSURE RECORDS FROM ARRAY TEST

MA-2553-62

27

Table 1

Time Interval Between Wavefront
Arrival and Edge Rarefaction Arrival

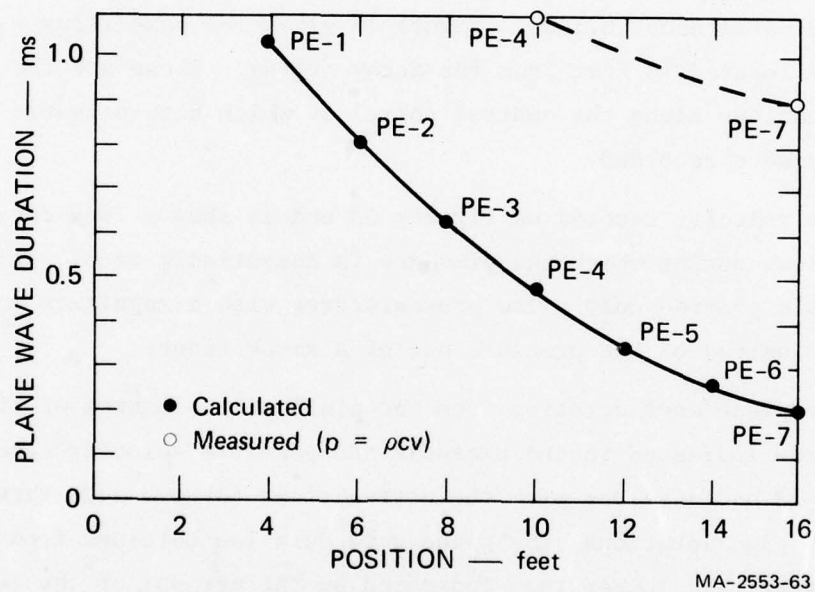| Gage Location	Distance from Array (ft)	Δt_p (ms)
1	4	1.035
2	6	0.812
3	8	0.629
4	10	0.490
5	12	0.349
6	14	0.276
7	16	0.209
8	10	0.493
9	10	0.492
10	10	0.481
11	10	0.251
12	10	0.088

FIGURE 12   PLANE WAVE DURATION FOR ARRAY TEST

Another way to determine plane wave duration is from the time interval over which the plane wave relation $p = \rho cv$ applies, where p is pressure, ρ is density, c is sound velocity, and v is particle velocity at corresponding times. Figure 13 illustrates this method for the gage located 16 feet from the array (PE-7). The upper record in Figure 13 is the pressure and the lower record is the velocity. The ratio $p/\rho cv$ at various times is given in the plot at the bottom. From the two straight lines in the figure we find that the plane wave relation is valid until about 6.1 ms. Figure 14 gives the same illustration for the gage located 10 feet from the array (PE-4). These are the only two gage locations along the central normal at which both pressure and velocity were recorded.

The velocity records of Figures 13 and 14 show a long-duration after-flow, during which the pressure is essentially zero. This after-flow would provide only a low pressure drag with a magnitude comparable to ρv^2, instead of the pressure ρcv of a shock front.

The plane wave duration from the plots at the bottom of Figures 13 and 14 are indicated in the pressure and particle velocity records of Figures 13 and 14 along with the arrival time for the edge rarefaction. For both gage locations, the plane wave duration obtained from the plots is substantially longer than indicated by the arrival of the edge rarefaction. This is attributed mainly to the finite rise time of the pulse from an individual source; the arrival time for the edge rarefaction is the earliest time that the missing line sources at the edge can be felt.

The plane wave duration from the plots of Figures 13 and 14 are plotted in Figure 12 (dashed line), along with the duration calculated from the arrival of the edge rarefaction. From Figure 12 we see that the plane wave durations from Figures 13 and 14 are about 1 ms, which is twice the rise time of the pulse. These results indicate that the effect of edge rarefactions on plane wave duration depends on the rise time of the pulse, as would be expected.
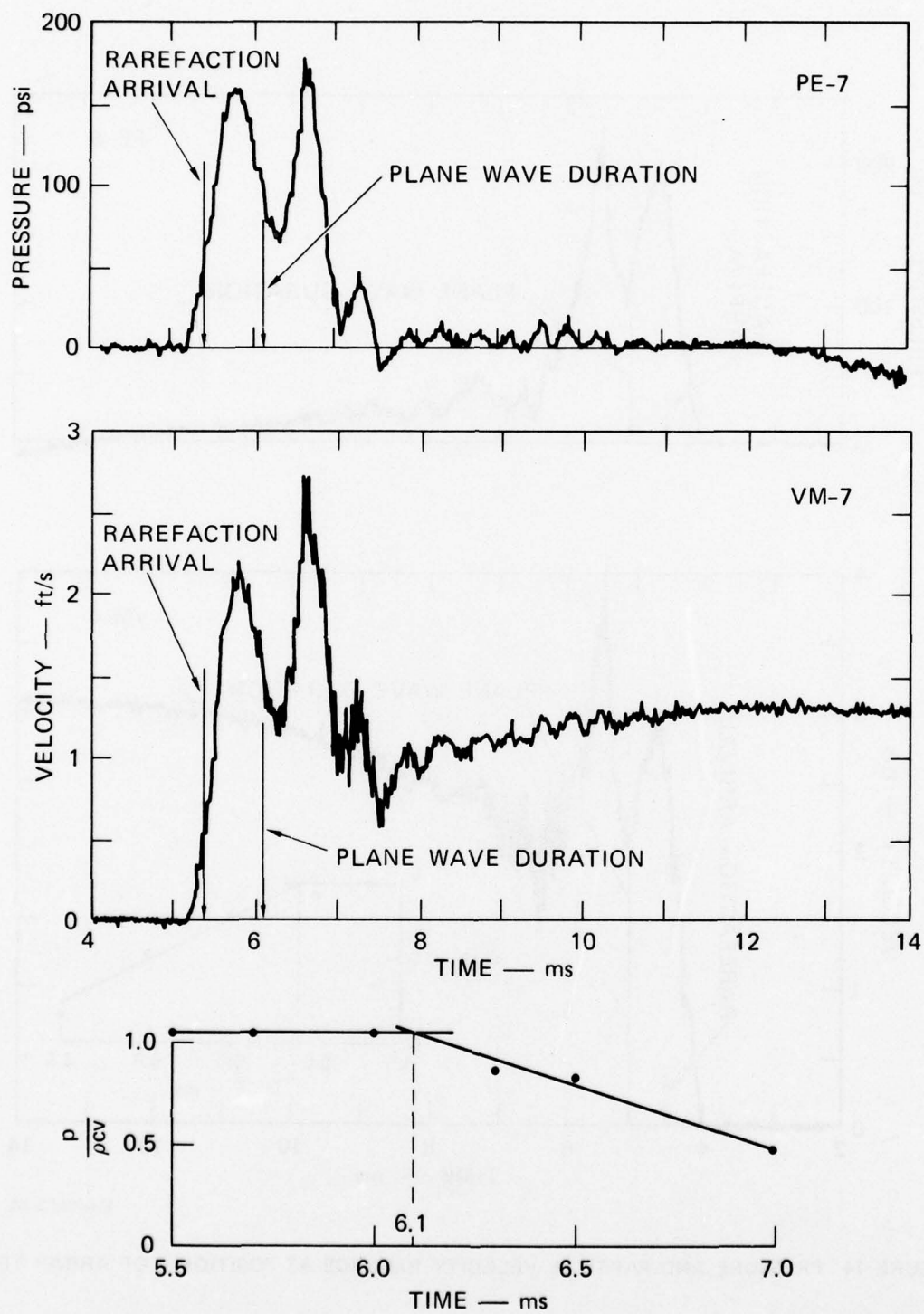
FIGURE 13   PRESSURE AND PARTICLE VELOCITY RECORDS AT POSITION 7
OF ARRAY TEST

31
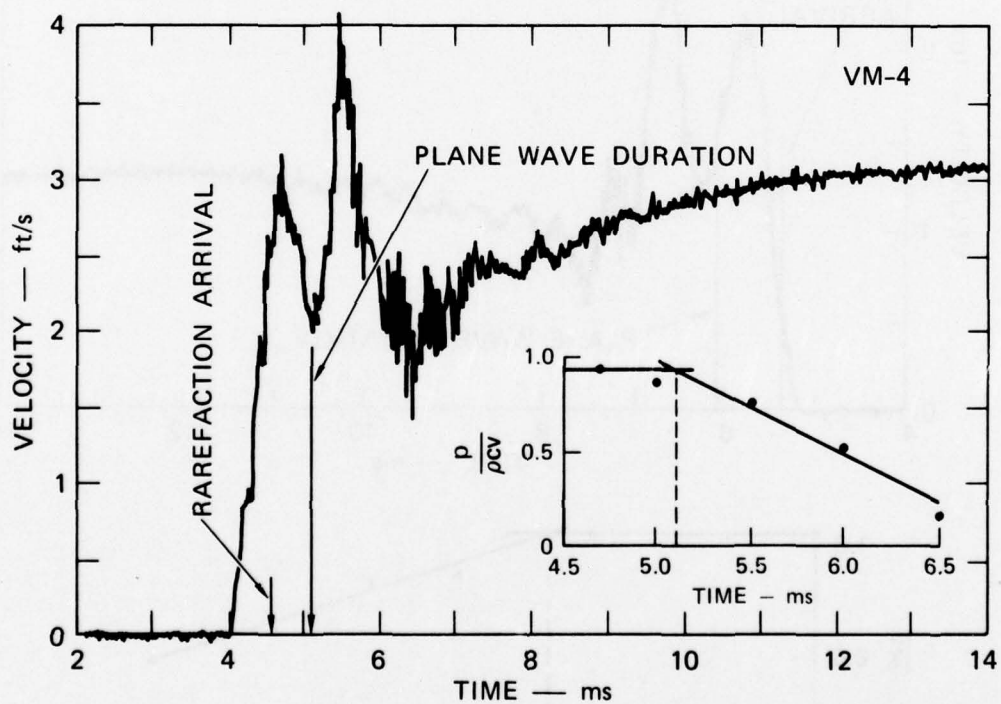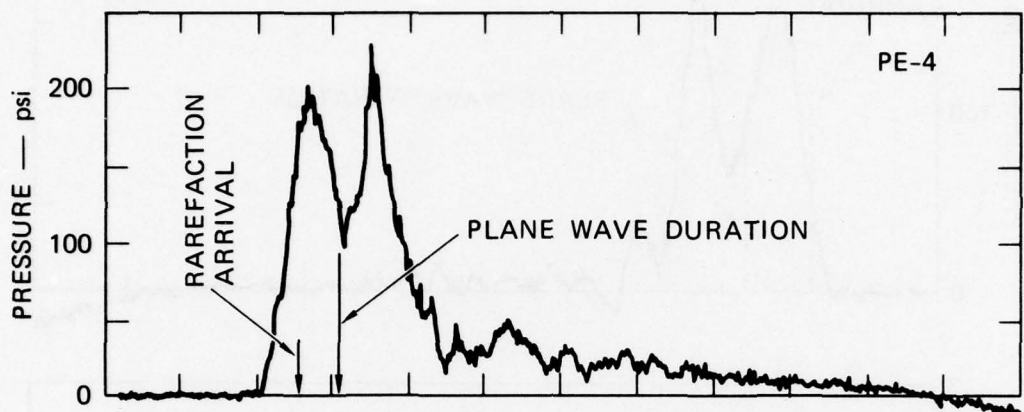
FIGURE 14 PRESSURE AND PARTICLE VELOCITY RECORDS AT POSITION 4 OF ARRAY TEST

MA-2553-65

32

The pressure records for the gage line running parallel to the array at a location 10 feet from the array are shown in Figure 15. As before, the spacing of the records is proportional to the spacing between gage locations. The record at the bottom of Figure 15 is the same as that at the middle of Figure 11. The records show the same general character as the records of Figure 11.

In Figure 15 we again show wavefront arrival time and rarefaction arrival time (calculated as indicated in Appendix B). Here we see that the time inverval between wavefront arrival time and rarefaction arrival time is approximately constant for the bottom three records and then falls off rapidly for the top two records. This time interval, plotted in Figure 16, is about 0.5 ms for the central gages.

Determination of the plane wave duration from the relation $p = \rho c v$, as done above for the gages along the central normal, results in the plots shown in Figures 17 and 18. Again we see that the plane wave duration determined from $p = \rho c v$ is substantially greater than indicated by rarefaction arrival.

From the preceding discussion we conclude that the array of point sources produced a plane wave with a duration, determined from the plane wave relation $p = \rho c v$, of about 1 ms along the central normal and longer at gage locations 9 and 12. The longer durations at gages 9 and 12 are not understood; they should be shorter than along the central normal.

Figure 19 shows the predicted relation between charge areal density and pressure and particle velocity that was developed from calibration tests from previous work.[2,3] In the array test, the charge loading density was 200 grains/ft. This corresponds to a charge areal density of 6.5 grains/ft^2. To determine the expected velocity and pressure from Figure 19, we first draw a horizontal line for an areal density of 6.5 grains/ft^2 over to line A. The abscissa value of the intersection of 4 ft/s is the corresponding velocity. The pressure is found by
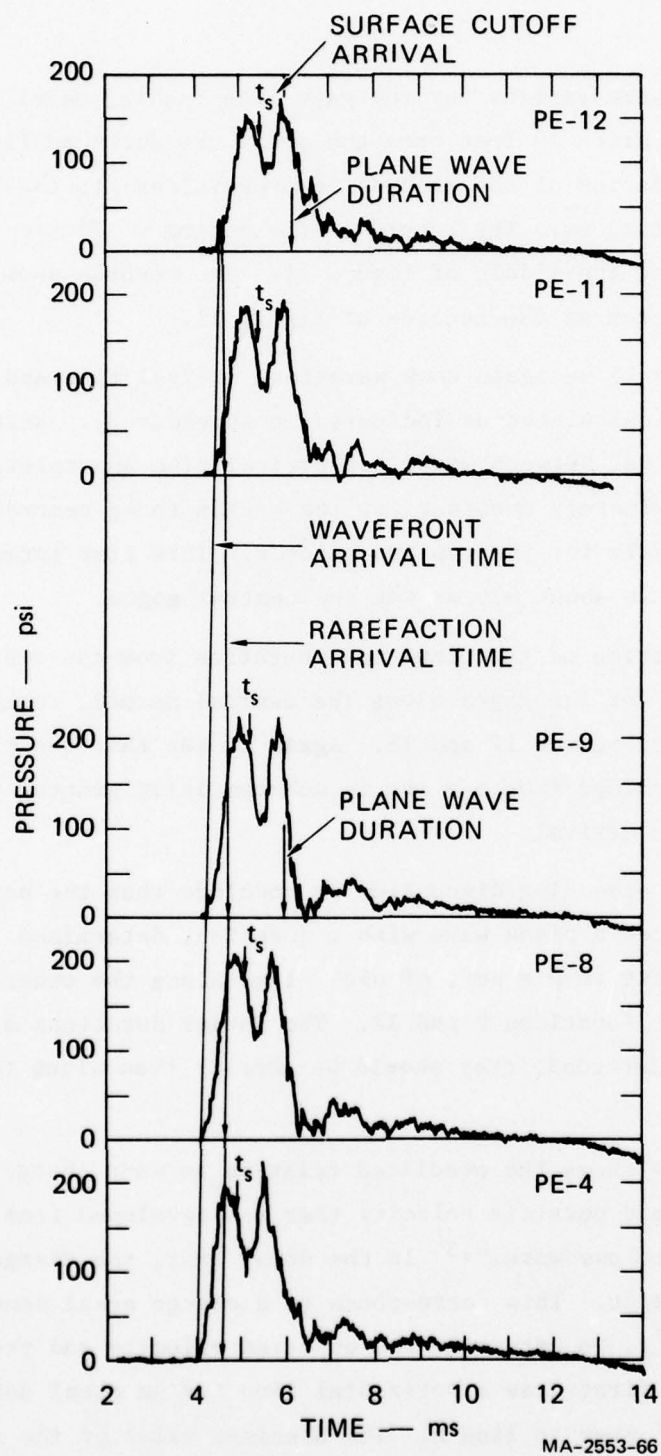
FIGURE 15   CROSS-AXIS PRESSURE RECORDS FROM
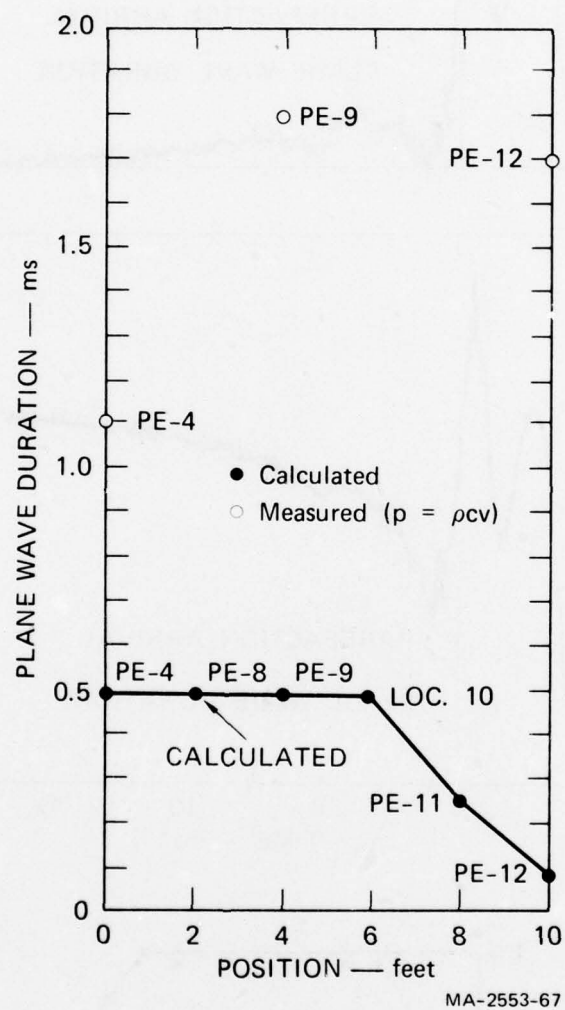ARRAY TEST

34

FIGURE 16 PLANE WAVE DURATION FROM
CROSS-AXIS MEASUREMENTS

35

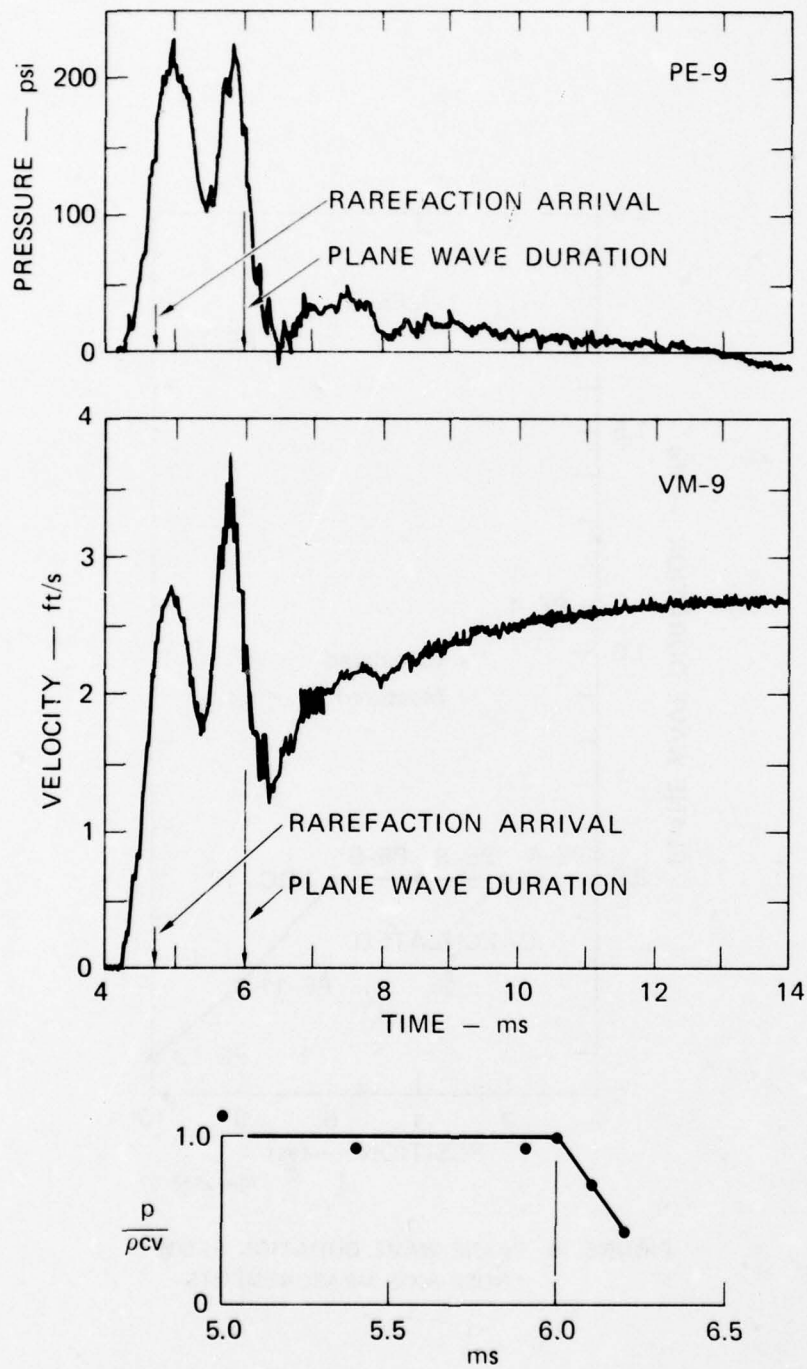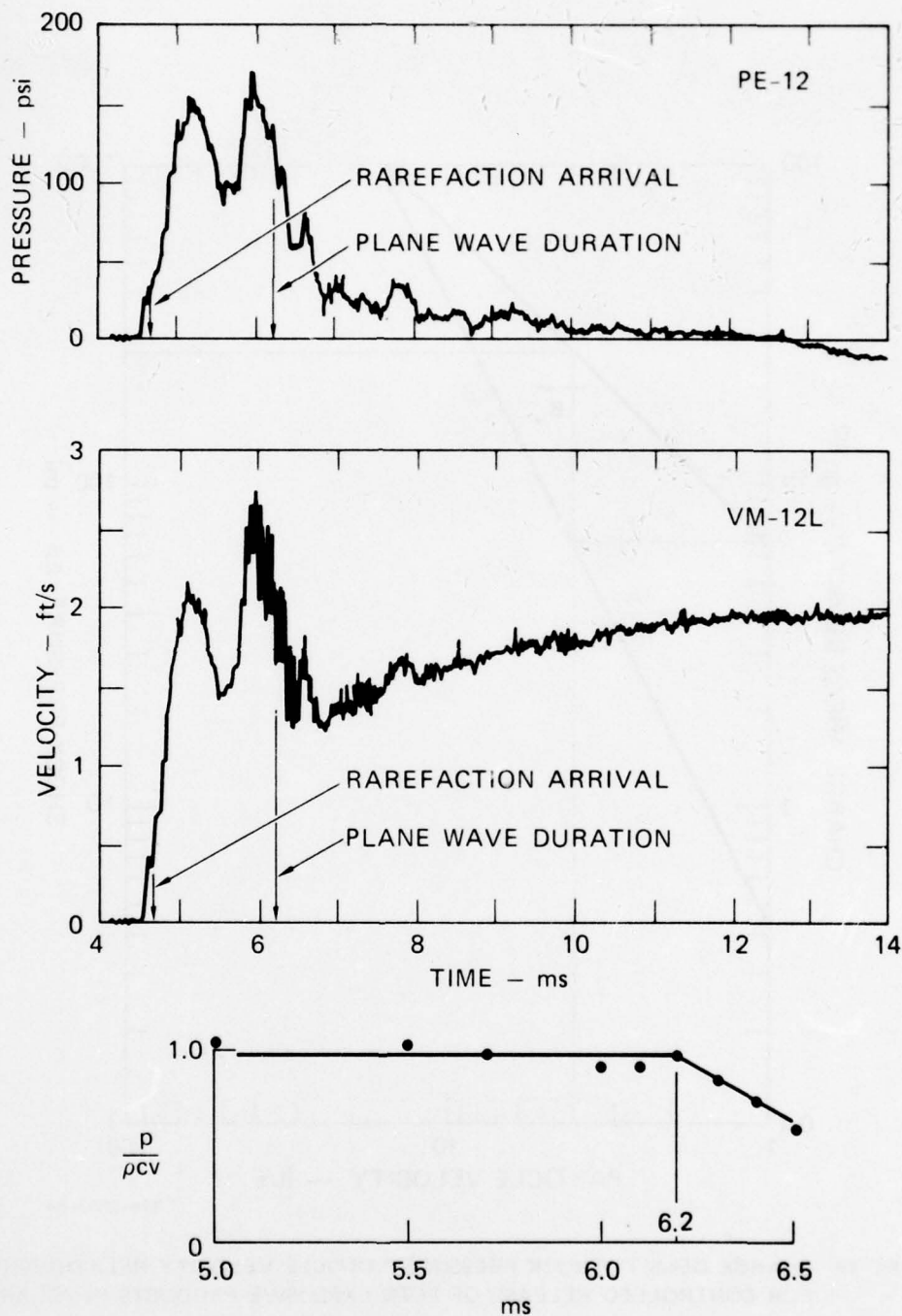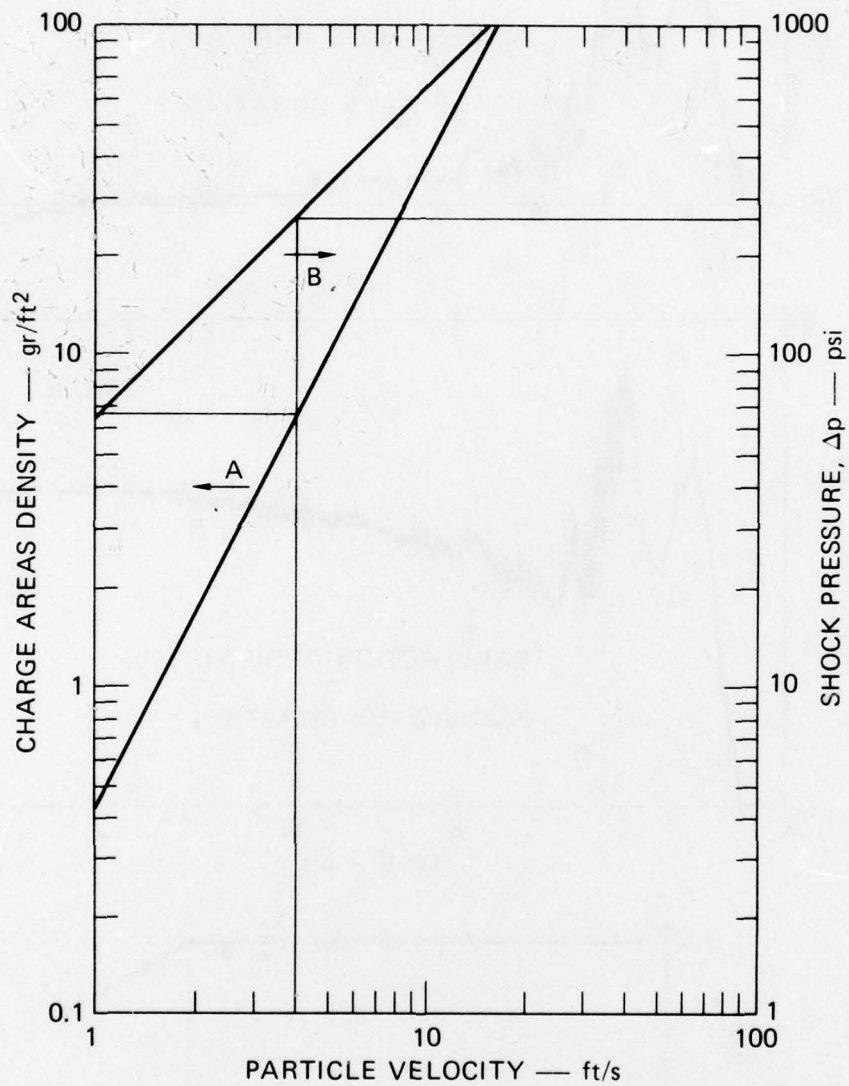FIGURE 17   PRESSURE AND PARTICLE VELOCITY RECORDS
AT POSITION 9 OF ARRAY TEST

FIGURE 18   PRESSURE AND PARTICLE VELOCITY RECORDS
AT POSITION 12 OF ARRAY TEST

MA-2553-34

FIGURE 19 CHARGE DENSITY/SHOCK PRESSURE/PARTICLE VELOCITY RELATIONSHIPS
FOR CONTROLLED RELEASE OF PETN EXPLOSIVE PRODUCTS IN AN ARRAY

extending a line upward from the intersection to curve B, and then reading the ordinate on the right. This gives a pressure of about 250 psi.

From Figure 14 we see that for gage location 4, which is 10 feet from the array, the particle velocity at the first peak is 3 ft/s and the pressure is 200 psi. These values occur just before the arrival of the edge rarefaction, and are well within the plane wave duration determined from $p = \rho c v$. Thus, velocity and pressure obtained are about 25% less than predicted. The difference is attributed to the greater surface available for bubble-water interaction in the array.

To test the validity of linear superposition of the pulses from the individual sources, we recorded the pulse from a single source, as shown in Figure 20(a). The method described in Appendix C, linear superposition of this pulse shape for the array, assuming 1/R attenuation, yields the plot for gage location 4 shown in Figure 20(b). Also shown is the measured pulse at gage location 4. We see that linear superposition gives a pressure that is over twice as large as the observed pressure. Hence we conclude that there is considerable interaction between the gas bubbles.

The characteristics of the pulse from a single source and those of the pulse from the array are compared in Figure 21. Both pulses shown are from gages located 4 feet from the sources. The rise time of the two pulses are the same, and the decay and second rise are similar. Hence it would appear possible to improve the pulse shape from the array by modifying the pulse shape from the individual sources. In particular, it should be possible to reduce the rise time of the array pulse by reducing the pulse rise time for the individual sources. To accomplish this, it would be best to start with high speed photography of an individual source so that the expansion characteristics of the valve bladder and bubble can be related to the features of the pressure record. One apparent way to minimize rise time is to minimize the initial volume within the bladder (see Figure 4).

39
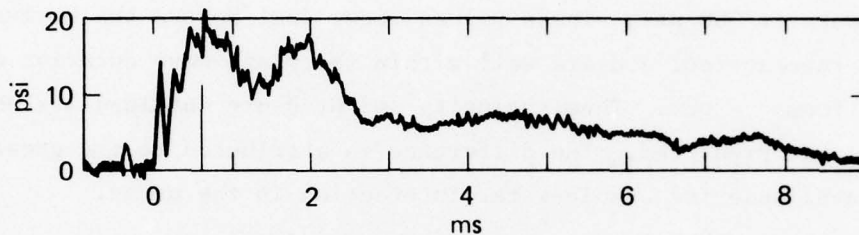
(a) PRESSURE PULSE MEASURED FROM UERD SINGLE
SOURCE, 4 FEET
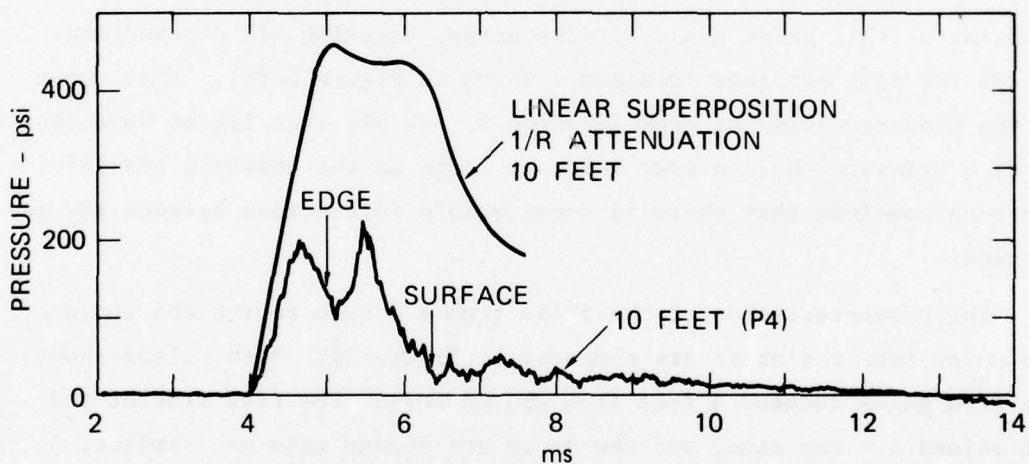
(b) LINEAR SUPERPOSITION OF PRESSURE PULSE AT
POSITION 4

MA-2553-70

FIGURE 20   EXPERIMENTAL AND THEORETICAL SUPERPOSITION RESULTS
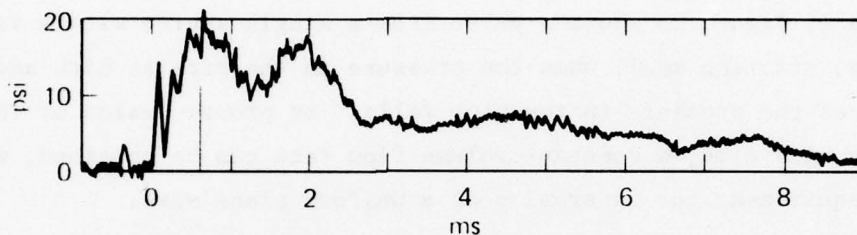
(a) PRESSURE PULSE MEASURED FROM UERD SINGLE SOURCE, 4 FEET
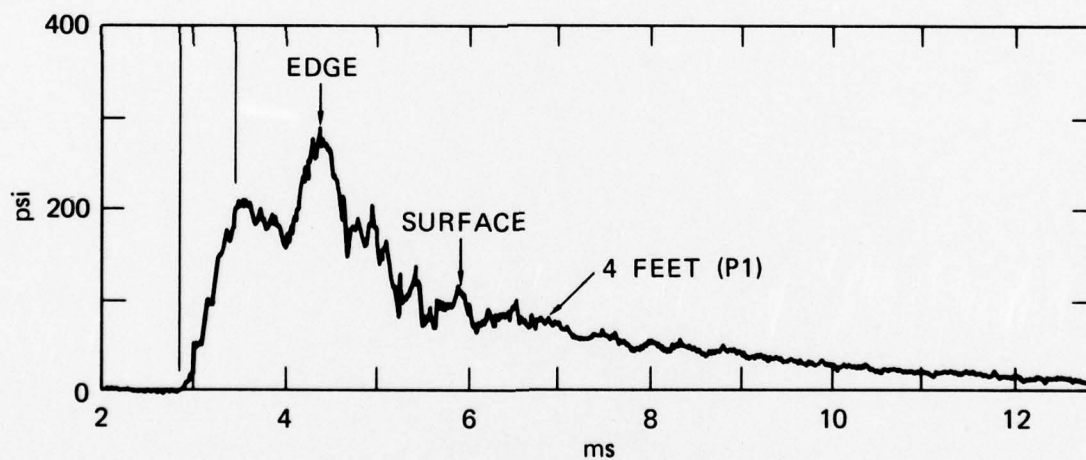
(b) PRESSURE PULSE MEASURED IN ARRAY TEST AT POSITION 1 (4 FEET)

MA-2553-71

FIGURE 21   EXPERIMENTAL SINGLE SOURCE AND SUPERPOSITION RESULTS AT 4 FEET

41

The two-peak characteristic of the pulses of Figure 21 is attributable at least in part to the initial vent area being greater than planned. Figure 22 shows a record from a single source for which the vent area was constant with time. In this case the two-peak feature is very severe. By contrast, Figure 23 shows a pulse from a single source with a variable vent area, starting small when the pressure in the pipe is high and increasing as the pressure in the pipe falls. By proper design of the vent area with time, a constant volume flow rate can be obtained, which is the requirement for generation of a uniform plane wave.
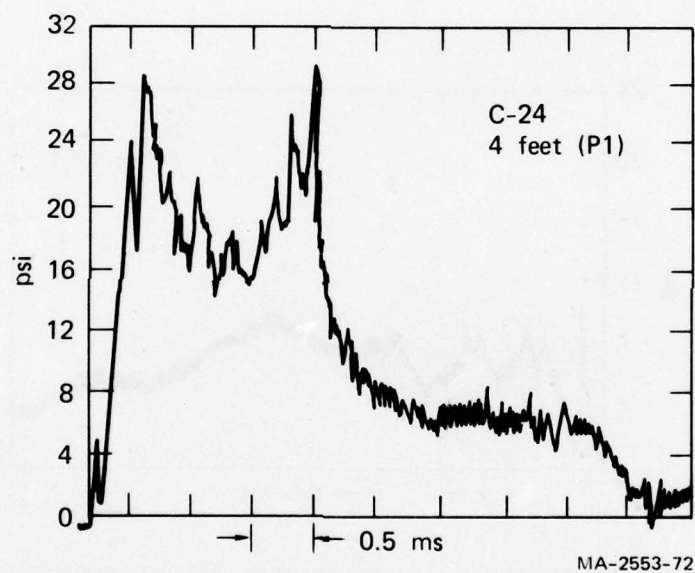
FIGURE 22 PRESSURE PULSE MEASURED AT HUNTERS POINT, USING SINGLE SOURCE WITH CONSTANT EXHAUST AREA

43
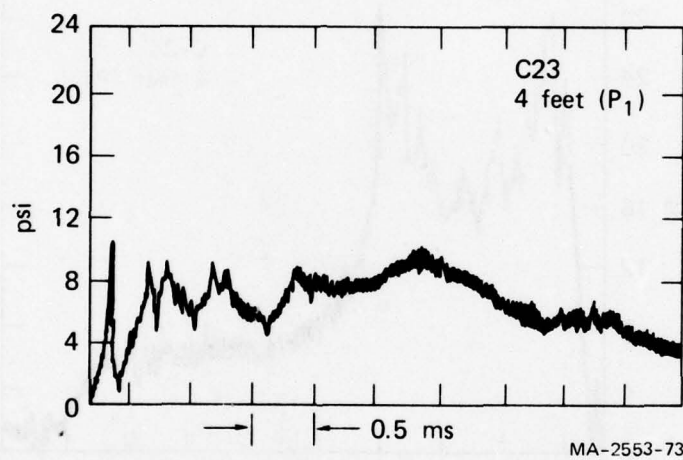
FIGURE 23 PRESSURE PULSE MEASURED AT HUNTERS POINT,
USING SINGLE SOURCE WITH INCREASING EXHAUST
AREA

Appendix A

ORIFICE VALVE AND ARRAY DEVELOPMEMENT

A key step in the development of the plane array technique described
in this report was the development of a practical, efficient valve that
releases gas at a constant volume rate for a desired pulse duration.
This appendix summarizes the experimental work performed during the
valve development program and describes the assembly of the valves into
an array.

Valve Design

Figure A-1 shows a cross section of the valve developed during
this program. The valve connects to an array pipe on the left. The
explosive gases enter the valve from the left and push on the piston.
Slots machined in the wall of the piston allow for gas exhaust. The
gas initially exhausts through the narrow part of the slot in the piston
wall and through the annular opening in the valve wall. As the piston
moves to the right, the exhaust area increases. The motion of the piston
is controlled by a fluid-orifice system. As the piston moves, it forces
fluid (oil) through orifices in the orifice plate. The motion of the
piston is controlled by adjusting the size of the orifice. After passing
through the orifice plate, the fluid compresses a volume of closed-cell
foam until the piston comes to rest. Then a spring in the fluid chamber
expands and pushes the piston back to its original position, and the
foam expands and displaces the fluid back into the fluid chamber. At
this point, the valve has returned to its original condition and is ready
for another test. This recocking feature makes the valve practical;
the valve need not be handled between tests.

FIGURE A-1 ORIFICE VALVE ASSEMBLY

MA-2553-57

Valve Motion Tests

Two types of tests were performed to evaluate the operation of this valve. In the first type, the motion of the piston as a function of time was measured, using an array of time-of-arrival pins mounted in the f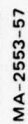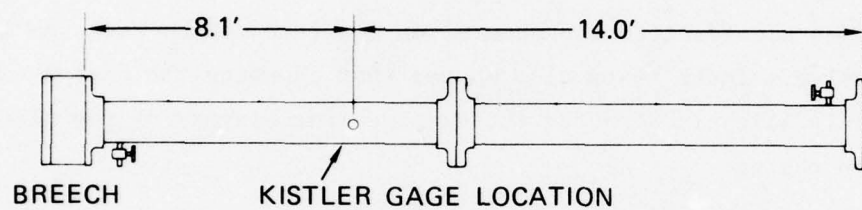luid chamber. These tests determined the charge required to move the piston 0.7 inch in 6 ms. Over this distance the exhaust area in the piston varies according to the theory for constant-volume-rate gas flow from the valve. These tests also showed that changing the piston exhaust geometry only slightly affected the displacement history of the piston for a given charge.

Valve Pulse Tests

In the second type of test, we measured the pressure pulse produced by the valve in the water-filled 22-foot-long, 6-inch-diameter pipe shown in Figure A-2. This pipe simulates a long, narrow column of water perpendicular to an array of these valves. Therefore, the pulse shape measured in the pipe will be similar to the pulse expected from an array of these valves. The valve was connected to a 2-foot-long, 2-inch-diameter pipe containing 2-foot-long charges of Primacord. The valve and connecting pipe were placed in the breech end of the 6-inch-diameter pipe.

The results from these tests are shown in Figure A-3. The pressure pulses were measured 8.1 feet from the breech end of the pipe. In each test, the charge and the orifice area that control piston motion were held constant, and the exhaust area of the piston as a function of displacement was varied. In Figure A-3(a), the exhaust area varied linearly with displacement; in Figure A-3(b), it varied as the displacement squared; and in Figure A-3(c), it varied approximately as displacement to the 2.5 power. The pressure rose abruptly to about 100 to 125 psi, remained fairly constant for 6 ms, and then decreased to atmospheric pressure as a relief wave from a free surface at the closed end of the pipe arrived at the gage. These three tests show that the valve produces volume at the desired constant rate and that the manner in which the

47

8.1'   14.0'

BREECH   KISTLER GAGE LOCATION

(a) TEST FIXTURE

2-INCH-DIAMETER PIPE

BLADDER

CHARGE
PIPE

6"

BREECH
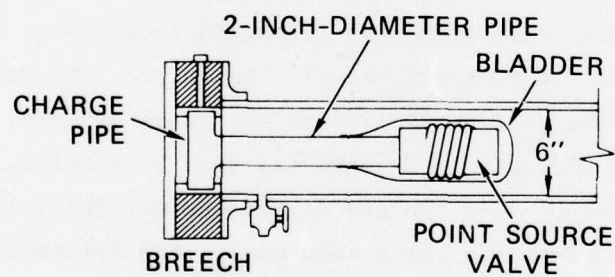
POINT SOURCE
VALVE

**(b) TEST CONFIGURATION OF POINT
VOLUME SOURCE**

MA–2553–45A

FIGURE A-2   EXPERIMENTAL SETUP TO TEST VALVES

(a)

$A_e \; \alpha \; x$

CHARGE = 100 grains
A_o = 1.24 cm^2
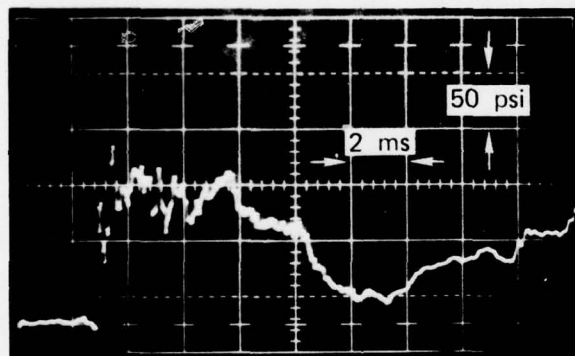
(b)
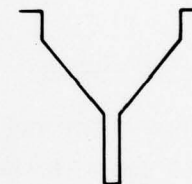
CHARGE = 100 grains
A_o = 1.24 cm^2

(c)

$A_e \; \alpha \; x^{2.5}$
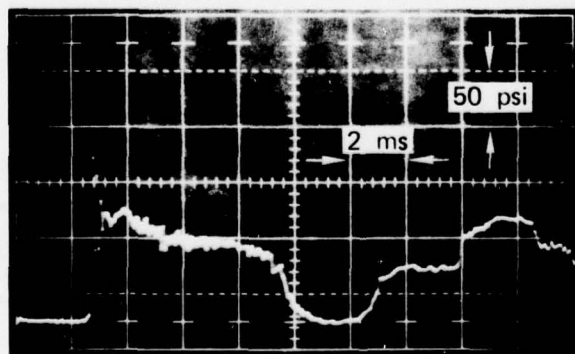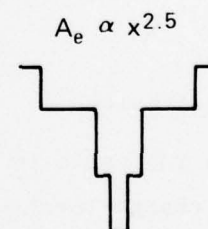
CHARGE = 100 grains
A_o = 1.24 cm^2

MP-2553-46

FIGURE A-3   EFFECT OF EXHAUST PORT GEOMETRY ON PRESSURE PULSE
SHAPE

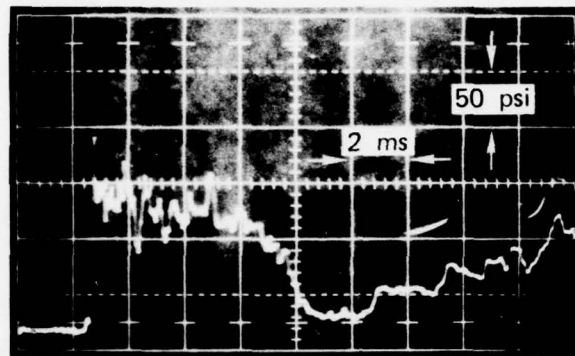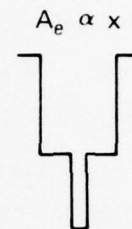exhaust port area increases with time is unimportant, provided a correctly chosen initial exhaust area is designed to increase by a factor of 4 after 6 ms. Therefore, in further tests, we used the simplest exhaust port geometry shown in Figure A-3(a).

In the test results shown in Figure A-3, the pressure was not as high as expected. The pressure was increased by placing a thick rubber bladder around the valve to prevent the exhaust gas from mixing with the water and losing energy through cooling. Figure A-4 shows two repeat tests with the same charge and valve geometry as in the tests without the bladder. The pressure now increases abruptly to 250 psi, twice that without the bladder, and remains constant for 6 ms before relieving to atmospheric pressure.

Variations in Charge

The next step was to see how the valve operated at other charge levels. To control the piston motion properly, we changed the orifice plate to provide a smaller orifice area for the large charge. The gas exhaust area in both tests is the same. Figure A-5 compares two pressure pulses produced at the different charge levels. The pressure for the larger charge now rises to about 900 psi before relieving to atmospheric pressure.

Valve Sensitivity

With the valve in this design, the orifice plate must be changed for each charge level to maintain the same exhaust area-time relationship. This feature means that the orifice plate would have to be changed each time a different peak shock pressure was required. To find a solution to this problem, we investigated the sensitivity of the pressure pulse to large changes in the charge level without changing the orifice plate. Figure A-6 shows pulses produced by the same valve at three charge levels. The peak pressure increases with charge level, as it should, but the pulse shape remains the same even for a factor of two increase over the

50
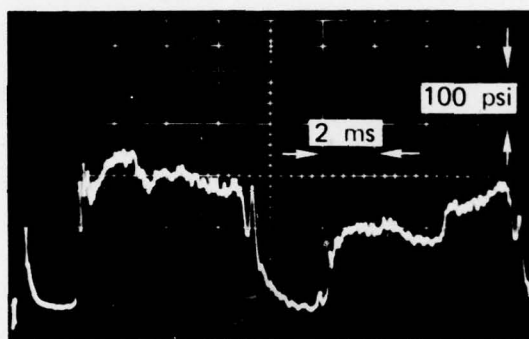
$A_e \ \alpha \ x$
CHARGE = 100 grains
A_o = 1.24 cm^2
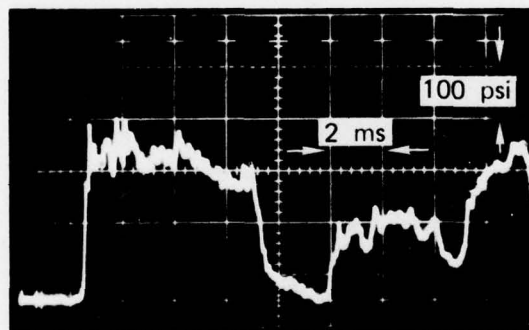
$A_e \ \alpha \ x$
CHARGE = 100 grains
A_o = 1.24 cm^2

MP-2553-47

FIGURE A-4   PRESSURE PULSE REPRODUCIBILITY

The valve is surrounded by a heavy rubber bag.

51

(a)

$A_e \, \alpha \, x$
$A_o = 1.24 \text{ cm}^2$
CHARGE = 100 grains

(b)

$A_e \, \alpha \, x$
$A_o = 0.60 \text{ cm}^2$
CHARGE = 400 grains
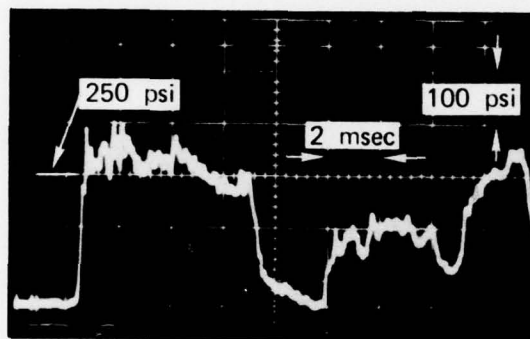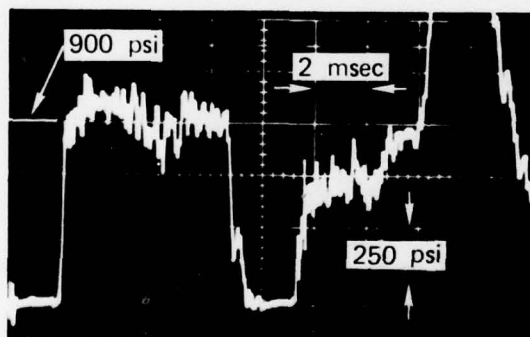
MP-2553-48

FIGURE A-5   PRESSURE PULSES PRODUCED BY VALVE AT NOMINAL
CHARGE LEVELS

52

250 psi

100 psi

2 msec

$A_e \propto x$
$A_o = 1.24 \text{ cm}^2$
CHARGE = 100 grains

(a) NOMINAL CHARGE

400 psi

250 psi

2 msec

$A_e \propto x$
$A_o = 1.24 \text{ cm}^2$
CHARGE = 150 grains

(b) 150% NOMINAL CHARGE

500 psi

250 psi

2 msec

$A_e \propto x$
$A_o = 1.24 \text{ cm}^2$
CHARGE = 200 grains
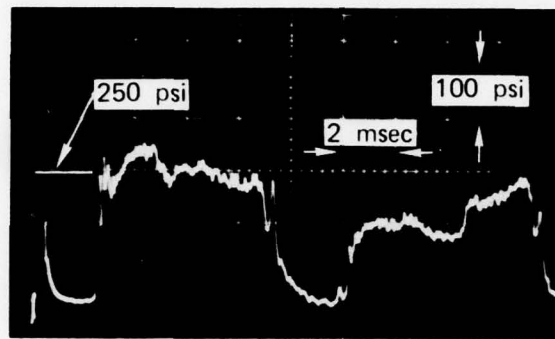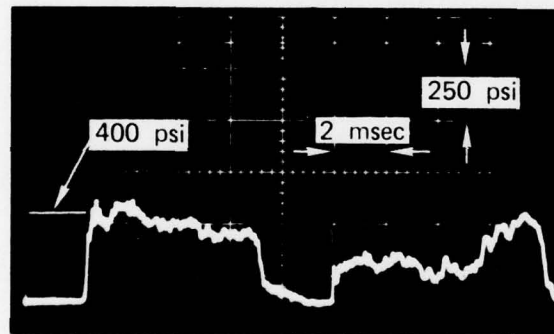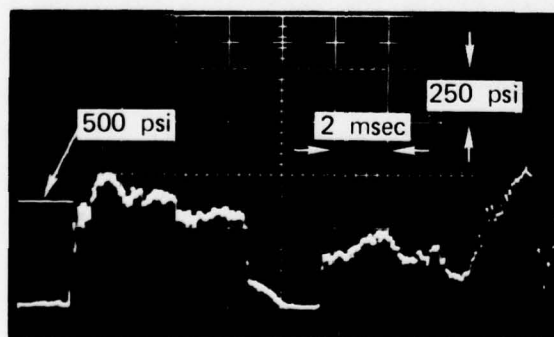
(c) 200% NOMINAL CHARGE

MP-2553-49

FIGURE A-6   EFFECT OF LARGE INCREASES IN NOMINAL DESIGN CHARGE
ON PRESSURE PULSE FOR FIXED ORIFICE PLATE

nominal design charge. A similar test was performed in which the charge was decreased to 50% of the design charge level. The results are shown in Figure A-7. Again, the pressure decreased as expected while the pulse shape remained the same.

To summarize the range of charge levels that can be used without affecting pulse shape, Figure A-8 shows a comparison between two pressure pulses produced by two valves with different control orifice plates. The charge level for each test is the same. However, each valve is operating at a charge level significantly different from the design charge level. In Figure A-8(a) the valve is operating at 50% of the nominal charge level, while in Figure A-8(b) the valve is operating at 200% of the nominal charge level. The pulses from both tests are remarkably similar. These tests suggest that a single valve would be capable of producing acceptable pulses for a factor of four change in charge level with the same control orifice plate. This fact, combined with the recocking feature, makes the valve practical for field use.

Bladder Design

One drawback of the valve design is that, upon submersion, the slots in the piston wall provide easy access for water into the valve and piping. To prevent flooding of the array between tests and to prevent the mixing and cooling of exhaust gages with the water during a test, a watertight, strong bladder encloses the valve. Several bladder designs were built and tested during the development period. Early in the bladder development work it was found that a steel baffle plate, shown in Figure A-9, was needed around the annular exhaust port of the valve to prevent the hot, high pressure gases from perforating the rubber bladder. This baffle forces the gases to vent axially out of the valve through slots in the annular orifice wall (Figure A-9).

The final bladder design, Figure A-10(a) includes a thick neoprene rubber tube that is clamped to the baffle plate. The other end of the tube forms a seal on the end plate of the valve to prevent water from
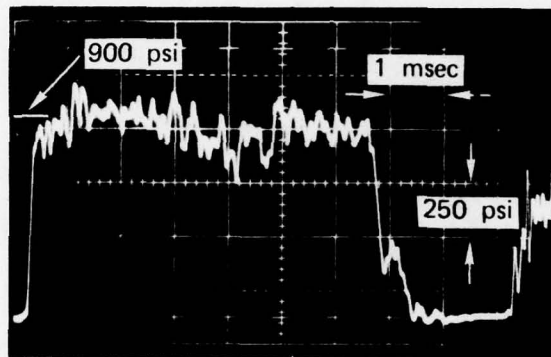
(a) NOMINAL CHARGE
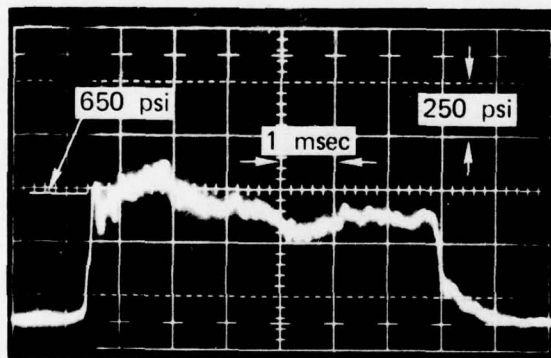
$A_e \propto x$
$A_o = 0.60 \text{ cm}^2$
CHARGE = 400 grains

(b) 50% NOMINAL CHARGE

$A_e \propto x$
$A_o = 0.60 \text{ cm}^2$
CHARGE = 200 grains

MP-2553-50

FIGURE A-7   EFFECT OF LARGE DECREASE IN NOMINAL DESIGN CHARGE
ON PRESSURE PULSE FOR FIXED ORIFICE PLATE

600 psi

1 msec

250 psi
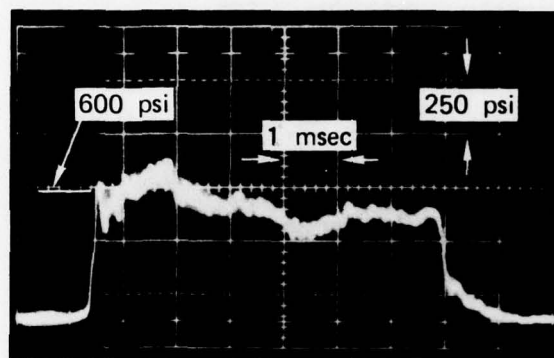
$A_e \propto x$
$A_o = 0.60\ cm^2$
CHARGE = 200 grains

(a) 50% NOMINAL CHARGE

600 psi

1 msec

250 psi
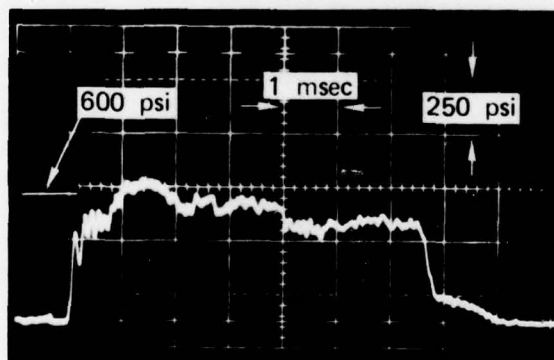
$A_e \propto x$
$A_o = 1.24\ cm^2$
CHARGE = 200 grains

(b) 200% NOMINAL CHARGE

MP-2553-51

FIGURE A-8   PRESSURE PULSES FROM VALVE WITH SAME CHARGE LEVEL
BUT DIFFERENT ORIFICE PLATES

GAS EXHAUST AREA
(4 PLACES)

BAFFLE

SECTION A-A

MA-2553-52

GAS EXHAUST

BAFFLE

A

A

TO ARRAY
PIPE
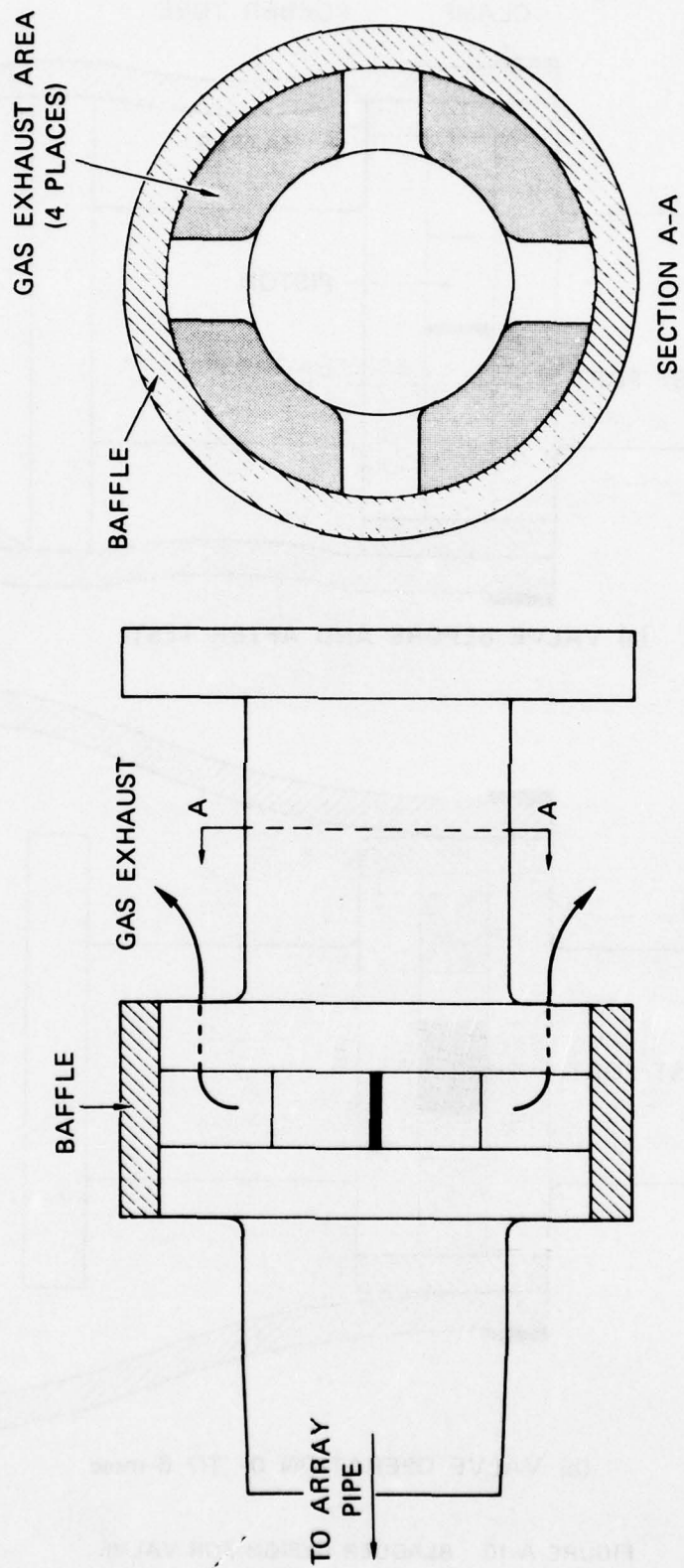
FIGURE A-9 BAFFLE DESIGN FOR VALVE

57

CLAMP   RUBBER TUBE

BAFFLE

TO ARRAY
PIPE

PISTON

EXHAUST PORT

SEAL
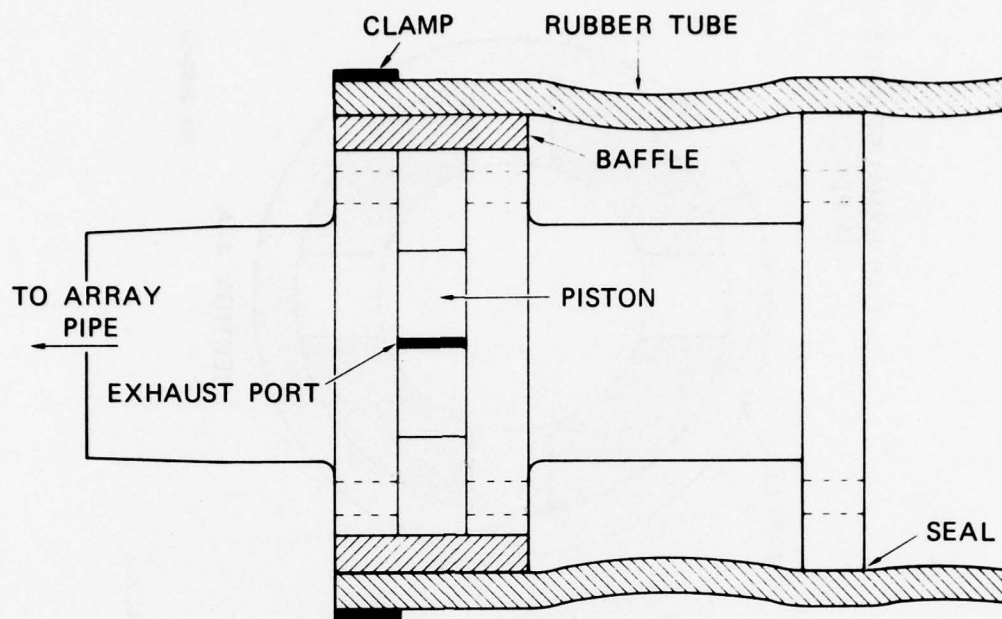
(a) VALVE BEFORE AND AFTER TEST

GASES

EXHAUST PORT
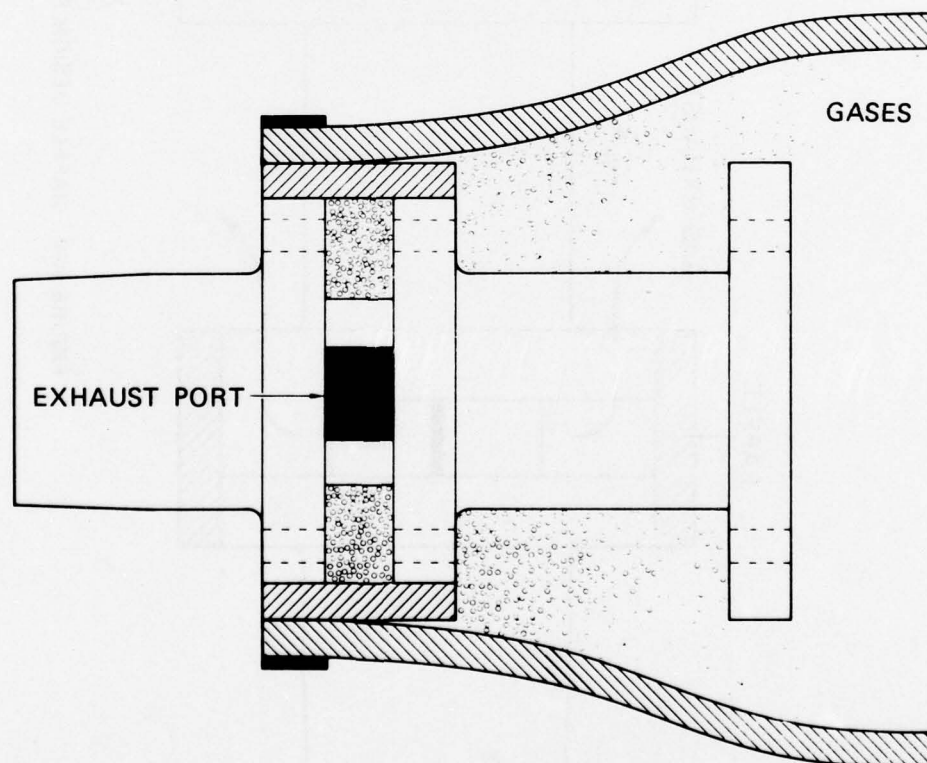
(b) VALVE OPERATION 0- TO 6-msec

MA-2553-53

FIGURE A-10   BLADDER DESIGN FOR VALVE

58

entering the valve. At first, when the gases exhaust from the valve, Figure A-10(b), the rubber tube expands, pushing on the water and producing the desired shock wave. The rubber tube prevents the gas and water from mixing during the early exhaust time. At late time the gases are expelled through the open end of the tube into the water. Then the rubber tube contracts to reseal the valve as shown in Figure A-10(a).

Array Design

Figure A-11 shows an engineering drawing of the typical elements in an array of the point source valves described above. Each array element is basically a 2-foot length of 2-inch, thick-walled, heat-treated steel pipe with high pressure, steel tees. The elements are welded together to form a line of point volume sources. The point source valves are screwed into each tee. The pipe and tees are wrapped in 1/4-inch-thick neoprene foam to prevent the shock-induced vibrations of the pipe elements caused by detonation of the explosive from producing undesirable pressure pulses. A pump is installed at the lower end of each array element to remove any water that might enter the piping system before the experiment. Primacord explosive is placed inside each array element. The explosive is detonated by a length of Primacord connected to the pieces of Primacord that extend out of the top of each array element.

This array design was used in the array tests described in this report. The array elements were supported by a floating shock platform that clamped each element so that about 2 feet of pipe extended above the water surface.

FIGURE A-11 ARRAY ELEMENT DESIGN

MA-2553-74

60

Appendix B

EDGE AND SURFACE EFFECTS

In this appendix we calculate the arrival time of the edge rarefaction and of the surface cutoff. The test configuration is such that the edge rarefaction arrives before surface cutoff, and hence determines the theoretical plane wave duration.

Figure B-1 shows the array layout. The hollow circles represent the array sources, the crosses are missing sources involved in determining arrival times of the edge rarefaction and surface cutoff, and the solid circles are gage locations.

The array source or missing source from which the signal arrives first at a gage location is not necessarily the nearest source, because sources nearer the initiation point start earlier. The detonation rate of the explosive is 22,620 ft/s (6900 m/s) and the wave speed in water is 5000 ft/s (1525 m/s). Thus, while the detonation travels the 2-foot distance between two sources, the wave from the first source travels 2(5000/22,620) = 0.44 foot in water. To find the source from which the signal arrives first at a given gage location, we calculate the distances from the sources to the gage location. The source from which the signal arrives first at the gage location is that which is less than 0.44 foot further from the gage location than the next closest source, and which is one 2-foot spacing closer to the initiation point than the next closest source.

Table B-1 gives the array source and missing edge source for first arrival at the various gage locations, the distances from the sources to the gage locations, and various time intervals of interest. The difference in wave transit times Δt_w to the gage location from the array source and the missing edge source is found by taking the difference between the distances to the gage location and dividing by the wave

61
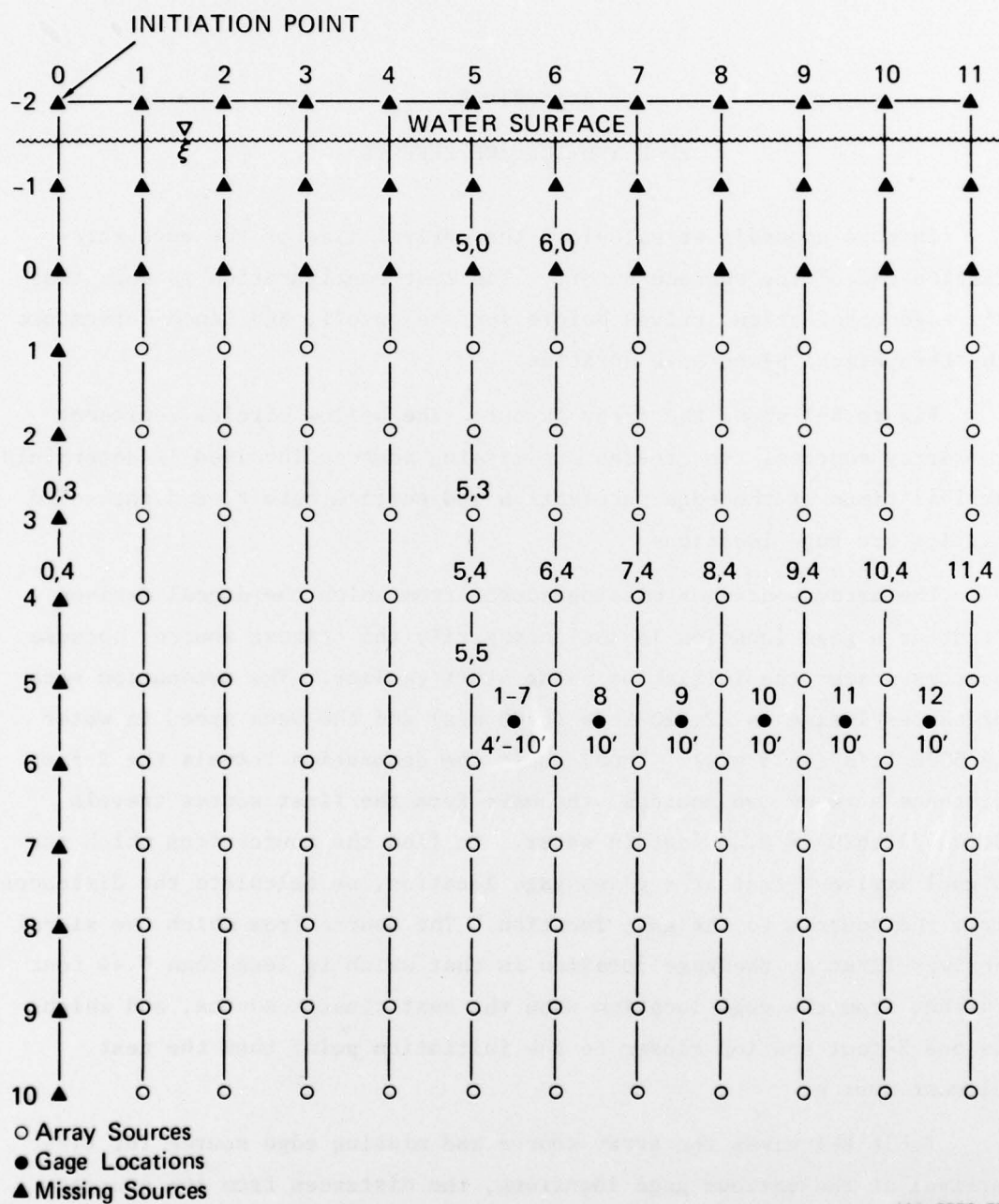
FIGURE B-1   ARRAY LAYOUT

MA-2553-75

62

Table B-1

ARRAY SOURCE AND MISSING EDGE SOURCE FOR FIRST ARRIVAL

AND THEORETICAL PLANE WAVE DURATION

Gage Loc.	Array Source			Missing Edge Source			Δt_w* (ms)	Δt_d* (ms)	Δt_p* (ms)
	Column	Row	Distance (feet)	Column	Row	Distance (feet)			
1	5	5	4.24	0	4	12.08	1.563	0.528	1.035
2	5	5	6.16	0	4	12.88	1.340	0.528	0.812
3	5	5	8.12	0	4	13.93	1.157	0.528	0.629
4	5	4	10.49	0	4	15.17	0.933	0.440	0.493
5	5	3	13.04	0	4	16.55	0.701	0.352	0.349
6	5	3	14.90	0	3	18.49	0.716	0.440	0.276
7	5	3	16.79	0	3	20.05	0.649	0.440	0.209
8	6	4	10.49	5	0	15.17	0.933	0.440	0.493
9	7	4	10.49	6	0	15.16	0.932	0.440	0.492
10	8	4	10.49	11	4	11.58	0.217	-0.264	0.481
11	9	4	10.49	11	4	10.86	0.075	-0.176	0.251
12	10	4	10.49	11	4	10.49	0	-0.088	0.088

*Δt_w = difference in wave transit times to gage location from array source and missing edge source.

Δt_d = difference in detonation arrival times at array source and missing edge source.

$\Delta t_p = \Delta t_w - \Delta t_d$ = theoretical plane wave duration.

speed in water 5000 ft/s (1525 m/s). The difference in detonation arrival time Δt_d is found by taking the distance between the array source and the missing edge source and dividing by the explosive detonation velocity. This time interval is positive if the missing edge source is closer to the initiation point than the array source. Then the plane wave duration is $\Delta t_p = \Delta t_w - \Delta t_d$. The values of Δt_p are plotted in Figures 11 and 15 as the rarefaction arrival time.

The surface cutoff time is found in a similar manner. As can be seen from Figure B-1, the missing sources that determine surface cutoff arrival are the sources in row -2. The sources in this row are the image sources for row -1. The signal from a source in row -1 must travel to the surface before the effect of the surface is apparent, and this is the same distance that the image source in row -2 must travel to reach the surface. Hence we can work with the image sources in row -2 in determining arrival times.

Table B-2 gives the array source (same as Table B-1) and the missing surface image source for first arrival, the distance from the sources to the gage locations, and the time intervals of interest. The surface cutoff times for gage locations 4 and 8 through 12 are the same, since they are all the same distance from the array and from the surface. The time intervals for surface cutoff Δt_s are plotted in Figures 11 and 15.

The water wave velocity can be found from the gage locations and arrival times along the gage line normal to the array. The distances and time intervals from gage location 1 are given in Table B-3. The average water wave velocity is 5000 ft/s (1525 m/s), in agreement with the handbook value of 1530 m/s.

To determine the detonation rate of the explosive, we use the arrival times at gage locations 4 and 12. Since these are the same distance from the array, the difference in arrival times is the time taken for the detonation to travel between the sources for which the signal arrives first at the gage locations.

64

Table B-2

SURFACE CUTOFF TIME

Gage Loc.	Array Source			Missing Image Source			Δt_w^* (ms)	Δt_d^* (ms)	Δt_s^* (ms)
	Column	Row	Distance (feet)	Column	Row	Distance (feet)			
1	5	5	4.24	4	-2	15.81	2.306	0.704	1.602
2	5	5	6.16	4	-2	16.43	2.143	0.704	1.439
3	5	5	8.12	4	-2	17.26	1.822	0.704	1.118
4	5	4	10.49	4	-2	18.28	1.552	0.616	0.936
5	5	3	13.04	3	-2	19.85	1.358	0.616	0.742
6	5	3	14.90	3	-2	21.12	1.240	0.616	0.624
7	5	3	16.79	3	-2	22.49	1.136	0.616	0.520
8	6	4	10.49	5	-2	18.28	1.552	0.616	0.936
9	7	4	10.49	6	-2	18.28	1.552	0.616	0.936
10	8	4	10.49	7	-2	18.28	1.552	0.616	0.936
11	9	4	10.49	8	-2	18.28	1.552	0.616	0.936
12	10	4	10.49	9	-2	18.28	1.552	0.616	0.936

*Δt_w, Δt_d same as in Table B-1.

$\Delta t_s = \Delta t_w - \Delta t_d$ = time interval from array signal arrival until surface signal arrival.

65

Table B-3

WAVE VELOCITY IN WATER

Gage Location	Distance From Loc. 1 (feet)	Interval* (ms)	Velocity† (ft/s)
1	0	0	--
2	2	0.40	5000
3	4	0.82	4878
4	6	1.20	5000
5	8	1.60	5000
6	10	1.96	5102
7	12	2.34	5128

*Time of arrival at gage location minus time of arrival at gage location 1.

†Average = 5000 ft/s.

66

From Table B-1 we see that the source for which the signal arrives first at gage location 4 is that in column 5 and row 4; for gage location 12, it is that in column 10 and row 4. From Figure B-1 we find that the extra distance the detonation must travel between these sources is 10 feet. From Figure 15, the difference in arrival times is 0.44 ms. This gives a detonation rate of 10 ft/0.44 ms = 22,727 ft/s ≈ 6900 m/s.

Appendix C

SUPERPOSITION CALCULATIONS

A summation routine was developed to add the pressure pulses gener-
ated by a single point source. The routine was used to calculate the
pressure pulse expected from a plane array of equally spaced point
sources. The summation routine assumed a linear superposition model
with a uniform pulse attenuation expected for a spherical source.
Figure C-1 shows the layout of the array of point sources and summarizes
the method for summing and pressure pulses. Shown in the figure is the
10×10 array of sources tested at UERD. The sources are spaced evenly
throughout the array at 2-foot intervals.

The principle of the superposition routine is to take a pressure
pulse from a single point source as measured in the free field and
assume that the pulse shape does not change with distance from the source.
The pulse is assumed to attenuate inversely with distance from the
source ($1/R$ attenuation). Since the single source measurement point and
the summation point do not, in general, coincide, the amplitude of the
pressure pulse from a single source is adjusted by a scale factor to
account for the difference in location between the single pulse measure-
ment point and the summation point. The scale factor obeys the attenu-
ation function and is given by $\phi = R/R_o$ where R is the distance from
the single source to the measurement point in the single valve experiment
and R_o is the normal distance from the array to the summation point
(see Figure C-1).

To simplify the summation routine, it is noticed that there are
two axes of symmetry in the array. Therefore, the summation considers
the sources in one quadrant only and multiplies the result by four. The
rows and columns of the array are subscripted from $i = 1$ to I and $J = 1$
to J, respectively. $I = 5$ and $J = 5$ for the UERD array. The pressure

69
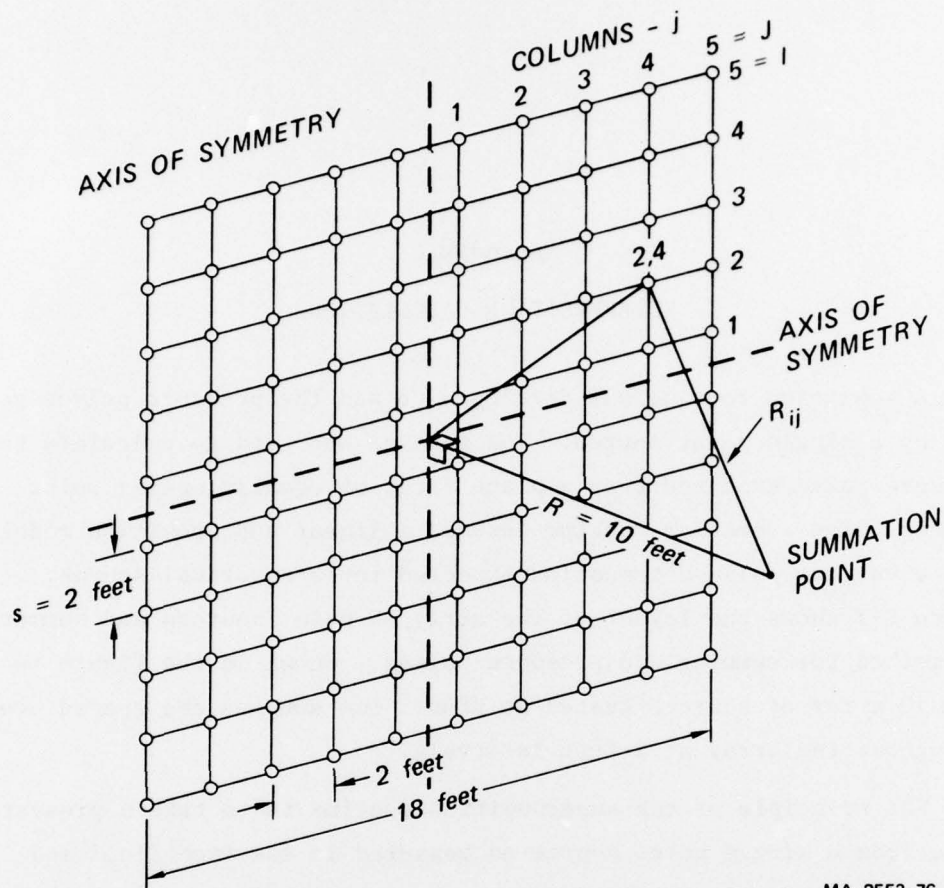
MA-2553-76

FIGURE C-1   GEOMETRY AND NOMENCLATURE USED IN SUPERPOSITION CALCULATIONS

$$R_{ij} = \left[\left[(i-1/2)^2 + (j-1/2)^2 \right] s^2 + R^2 \right]^{1/2}$$

$t_{ij} = \dfrac{R_{ij}}{c}$ = TIME OF ARRIVAL OF PULSE AT SUMMATION POINT
AND c = SPEED OF SOUND IN WATER

for $t \geq t_{ij}$

$$P_o(t) = \sum_{i=1, j=1}^{I=5, J=5} 4 \frac{R}{R_{ij}} \phi p(t-t_{ij})$$

ϕ = SCALE FACTOR $\dfrac{R_s}{R}$

WHERE R_s = DISTANCE FROM SOURCE TO MEASUREMENT POINT
IN SINGLE SOURCE TESTS

R   = DISTANCE FROM ARRAY TO SUMMATION POINT

$p(t-t_{ij})$ = PULSE SHAPE OF SINGLE POINT SOURCE

70

pulses from each source in the quadrant arrive at the summation point sequentially as i and j increase. The time of arrival of the pressure pulse from each source at the summation point is $t_{ij} = R_{ij}/c$ where c is the speed of sound in water and R_{ij} is the distance from the source to the summation point given by the expression:

$$R_{ij} = \left\{ [(i - 1/2)^2 + (j - 1/2)^2]S^2 + R_o^2 \right\}^{\frac{1}{2}}$$

where S is the source spacing. The amplitude of the pressure pulse from each source attenuates from a pressure $P = p\phi$ to a lower pressure $P_o = (R_o/R_{ij})\phi p$, where p is the pressure pulse measured in the single source experiment and ϕ is the scale factor discussed above. The summation routine determines for each time step (0.04 ms) which sources are acting at the summation point ($t \geq t_{ij}$) and then sums the pressure using the following formula:

$$P_o(t) = \sum_{i=1,j=1}^{I,J} 4 \frac{R_o}{R_{ij}} \phi p(t - t_{ij}) \qquad t \geq t_{ij}$$

Values of $p(t - t_{ij})$ are interpolated from an input table of the pressure-time history of the pulse from a single source. Figure C-2(a) shows the pulse from a single source measured 4 feet from the source in an experiment carried out at UERD. Also shown are the points used in tabulating the pressure data. The summation was performed at a standoff distance of 10 feet from the 10 x 10 array tested at UERD (ϕ = 0.4). The summation result is shown in Figure C-2(b) along with the pressure pulse measured 10 feet from the 10 x 10 array.

A few important points must be considered when comparing the superposition results with the experimental results. First, the superposition calculation assumes that all point sources in the array generate pressure waves at the same time where, as described in the body of this report, the point source valves begin operation sequentially because of the

71
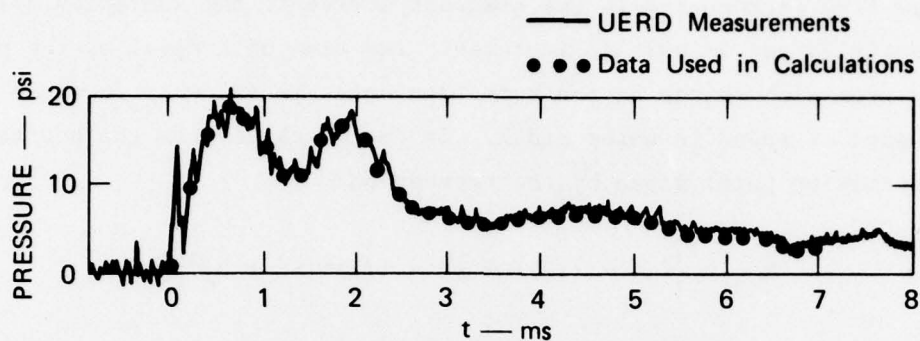
(a) UERD SINGLE SOURCE — 4 feet
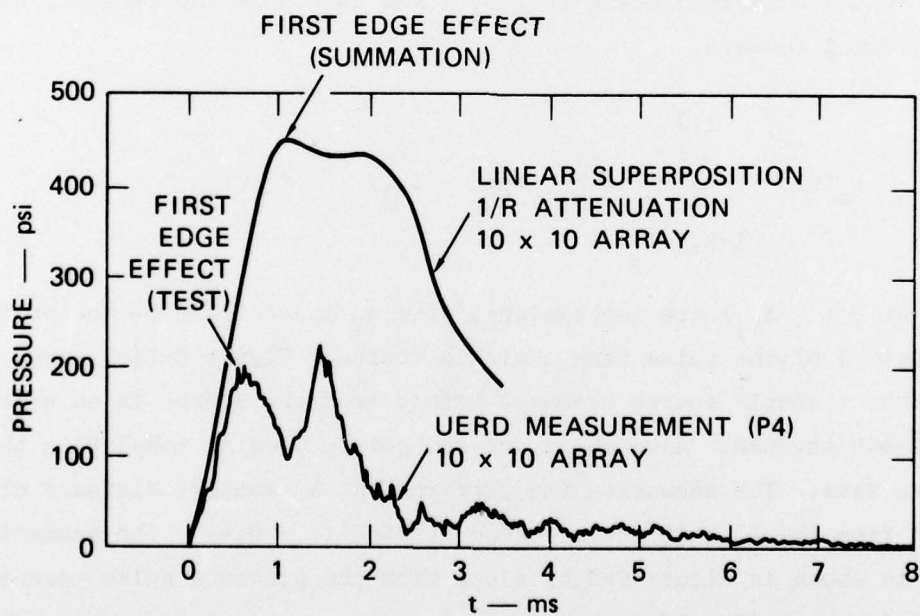
(b) PRESSURE PULSES 10 FEET AWAY FROM ARRAY

MA-2553-77

FIGURE C-2   PRESSURE PULSES USED IN SUPERPOSITION CALCULATIONS

explosive initiation technique. Second, both the experiment and analysis display edge effects. However, the edge effects for the analysis arrive later than those in the experiment, again because of the explosive initiation technique. The first missing edge source in the experiment arrives at the measurement point (gage 4) 0.493 ms after pulse arrival time (see Table B-1 in Appendix B). The first missing edge source in the analysis arrives at the summation point 0.972 ms after pulse arrival time. As mentioned in the body of the report, edge effects do not rapidly reduce the pressure because of the rather long, gradual rise time of the source pulse.

DISTRIBUTION LIST

DEPARTMENT OF DEFENSE

Assistant to the Secretary of Defense
Atomic Energy
    ATTN: ATSD (AE)

Director
Defense Advanced Rsch. Proj. Agency
    ATTN: Technical Library
    ATTN: NMRO
    ATTN: PMO
    ATTN: STO

Director
Defense Civil Preparedness Agency
    ATTN: Admin. Officer

Defense Documentation Center
Cameron Station
12 cy ATTN: TC

Director
Defense Intelligence Agency
    ATTN: DB-4C, E. O'Farrell
    ATTN: DT-1C
    ATTN: DT-2, Wpns. & Sys. Div.

Director
Defense Nuclear Agency
    ATTN: TISI
    ATTN: DDST
2 cy ATTN: SPSS
3 cy ATTN: TITL

Chairman
Dept. of Defense Explo. Safety Board
    ATTN: T. Zaker
    ATTN: DD/S&SS

Commander
Field Command, Defense Nuclear Agency
    ATTN: FCPR
    ATTN: FCT
    ATTN: FCTMOF

Chief
Livermore Division, Fld. Command, DNA
    ATTN: FCPRL

Commandant
NATO School (SHAPE)
    ATTN: U.S. Documents Officer

Chief
Test Construction Division
Field Command Test Directorate
    ATTN: FCTC

Under Sec'y of Def. for Rsch. & Engrg.
    ATTN: S&SS (OS)

DEPARTMENT OF THE ARMY

Dep. Chief of Staff for Rsch. Dev. & Acq.
    ATTN: Technical Library

DEPARTMENT OF THE ARMY (Continued)

Chief of Engineers
    ATTN: DAEN-MCE-D
    ATTN: DAEN-RDM

Deputy Chief of Staff for Ops. & Plans
    ATTN: Technical Library

Commander
Harry Diamond Laboratories
    ATTN: DELHD-NP
    ATTN: DELHD-TI, Technical Library

Commander
Redstone Scientific Information Ctr.
    ATTN: Chief, Documents

Director
U.S. Army Ballistic Research Labs.
    ATTN: DRDAR-BLE, W. Taylor
    ATTN: DRXBR-X, J. Meszaros
    ATTN: DRDAR-BLE, J. Keefer
    ATTN: Tech. Library, E. Baicy

Director
U.S. Army Engr. Waterways Exper. Sta.
    ATTN: G. Jackson
    ATTN: J. Strange
    ATTN: Technical Library
    ATTN: W. Flathau

Commander
U.S. Army Mat. & Mechanics Rsch. Ctr.
    ATTN: Technical Library

Commander
U.S. Army Materiel Dev. & Readiness Cmd.
    ATTN: Technical Library

Commander
U.S. Army Mobility Equip. R&D Ctr.
    ATTN: Technical Library

Commander
U.S. Army Nuclear & Chemical Agency
    ATTN: Library

DEPARTMENT OF THE NAVY

Chief of Naval Material
    ATTN: MAT 0323

Chief of Naval Operations
    ATTN: OP 981
    ATTN: OP 03EG

Chief of Naval Research
    ATTN: Code 461, J. Warner
    ATTN: Code 464, T. Quinn
    ATTN: Code 474, N. Perrone
    ATTN: Technical Library

Commander, Naval Elec. Sys. Command
    ATTN: PME, 117-21A

DEPARTMENT OF THE NAVY (Continued)

Officer-in-Charge
Civil Engineering Laboratory
     ATTN: R. Odello
     ATTN: Technical Library

Commander
David W. Taylor Naval Ship R&D Ctr.
     ATTN: Code L42-3, Library
     ATTN: Code 17
     ATTN: Code 1740.1
2 cy ATTN: Code 177
2 cy ATTN: Code 1740.5

Commander
Naval Facilities Engineering Command
     ATTN: Code 03A
     ATTN: Technical Library
     ATTN: Code 04B

Director
Naval Research Laboratory
     ATTN: Code 2600, Technical Library
     ATTN: Code 8440, G. O'Hara

Commander
Naval Sea Systems Command
     ATTN: Code 03511
     ATTN: ORD-91313, Library

Commander
Naval Ship Engineering Center
     ATTN: Technical Library
3 cy ATTN: NSEC 6105

Officer-in-Charge
Naval Surface Weapons Center
     ATTN: Code WA501, Navy Nuc. Prgms. Off.
     ATTN: Dr. Blatstein

Commander
Naval Surface Weapons Center
Dahlgren Laboratory
     ATTN: Technical Library

Director
Strategic Systems Project Office
     ATTN: NSP-272
     ATTN: NSP-43, Technical Library

DEPARTMENT OF THE AIR FORCE

AF Geophysics Laboratory, AFSC
     ATTN: LWW, K. Thompson

AF Institute of Technology, AU
     ATTN: Library, AFIT Bldg. 640, Area B

AF Weapons Laboratory, AFSC
     ATTN: DES-S, M. Plamondon
     ATTN: DES-C, R. Henny
     ATTN: SUL
     ATTN: DEX

Headquarters
Air Force Systems Command
     ATTN: DLCAW

HQ USAF/IN
     ATTN: INATA

DEPARTMENT OF THE AIR FORCE (Continued)

HQ USAF/RD
     ATTN: RDQSM

Commander in Chief
Strategic Air Command
     ATTN: NRI-STINFO Library

DEPARTMENT OF ENERGY

Albuquerque Operations Office
     ATTN: Doc. Con. for Technical Library

Division of Headquarters Services
     ATTN: Doc. Con. for Class Tech. Lib.

Nevada Operations Office
     ATTN: Doc. Con. for Tech. Lib.

Division of Military Application
     ATTN: Doc. Con. for Test Office

University of California
Lawrence Livermore Laboratory
     ATTN: Doc. Con. for L-96, L. Woodruff
     ATTN: Doc. Con. for L-3, Tech. Info. Dept.

Los Alamos Scientific Laboratory
     ATTN: Doc. Con. for Reports Lib.

Sandia Laboratories
Livermore Laboratory
     ATTN: Doc. Con. for Tech. Library

Sandia Laboratories
     ATTN: Doc. Con. for 3141, Sandia Rpt. Coll.

DEPARTMENT OF DEFENSE CONTRACTORS

Aerospace Corp.
     ATTN: Tech. Info. Services

Boeing Co.
     ATTN: Aerospace Library

Civil/Nuclear Systems Corp.
     ATTN: R. Crawford

EG&G Washington Analytical Services Center, Inc.
     ATTN: Technical Library

General Electric Co.-TEMPO
Center for Advanced Studies
     ATTN: DASIAC

IIT Research Institute
     ATTN: Technical Library

Institute for Defense Analyses
     ATTN: IDA Librarian, R. Smith

Kaman Sciences Corp.
     ATTN: Library

Lockheed Missiles & Space Co., Inc.
     ATTN: Technical Library

Lockheed Missiles & Space Co., Inc.
     ATTN: Technical Library
     ATTN: T. Geers

DEPARTMENT OF DEFENSE CONTRACTORS (Continued)

Physics International Co.
    ATTN: C. Vincent
    ATTN: E. Moore
    ATTN: Technical Library

Pacifica Technology
2 cy ATTN: J. Kent

R&D Associates
    ATTN: R. Port
    ATTN: J. Lewis
    ATTN: Technical Library

Science Applications, Inc.
    ATTN: Technical Library

Science Applications, Inc.
    ATTN: R. Shunk

Southwest Research Institute
    ATTN: A. Wenzel
    ATTN: W. Baker

SRI International
    ATTN: G. Abrahamson
    ATTN: B. Gasten
    ATTN: C. Romander

DEPARTMENT OF DEFENSE CONTRACTORS (Continued)

Systems, Science & Software, Inc.
    ATTN: D. Grine
    ATTN: Technical Library

TRW Defense & Space Sys. Group
    ATTN: Tech. Info. Center
    ATTN: D. Baer
2 cy ATTN: P. Dai

TRW Defense & Space Sys. Group
San Bernardino Operations
    ATTN: E. Wong

The Eric H. Wang
Civil Engineering Rsch. Fac.
University Station
    ATTN: N. Baum
    ATTN: L. Bickle

Weidlinger Assoc., Consulting Engineers
    ATTN: M. Baron

Weidlinger Assoc., Consulting Engineers
    ATTN: J. Isenberg